UNIVERSITAT POLITÈCNICA DE CATALUNYA

Programa de Doctorat Recursos Naturals i Medi Ambient

STUDY OF DENITRIFICATION AND REDUCTIVE DECHLORINATION PROCESSES APPLIED TO GROUNDWATER BIOREMEDIATION

Ph.D. thesis

Montse Calderer Perich

Supervised by

Joan de Pablo Ribas

Vicenç Martí Gregorio

MANRESA, April 2010

PART I - Chapter 5

STUDY OF THE DENITRIFICATION PROCESS UNDER DYNAMIC EXPERIMENTAL CONDITIONS

1. INTRODUCTION

The denitrification rate and efficiency are site-specific and it is known that they are often limited by a wide range of environmental factors such as the microbial population, the pH, the temperature, the oxygen content and the availability of electron donors. Therefore, to better assess the potential of *in situ* bioremediation of nitrate, studies incorporating flow conditions and identifying the limiting factors are needed. In addition, as mentioned in Chapter 1, another important issue to perform *in situ* field tests is the application of mathematical models to determine biological reaction rates coupled with physical processes involved in aquifers (Lensing *et al.*, 1994; Zhao *et al.*, 2003).

Until now, the complexity of groundwater systems has prevented the application of *in situ* treatments to remediate nitrate contamination and, relatively few attempts have been reported worldwide. Many of these studies involved injecting a soluble substrate into an aquifer and withdraw treated water using a particular configuration of wells (Khan and Spalding, 2003; 2004; Smith *et al.*, 2001). In a different approach, some works have applied Permeable Reactive Barriers (PRBs) to *in situ* treat nitrate-contaminated groundwater (Robertson *et al.*, 2000; Schipper *et al.*, 2004). The LIFE Environment Project NITRABAR (NITRABAR, 2009) developed a system based on PRBs containing a mixture of natural material to remove nitrate from shallow groundwater. The project demonstrated the feasibility of the technology at a site in Northern Ireland at which subsurface nitrate concentrations were reduced by over 90%.

At laboratory scale, numerous authors have investigated the denitrification process under dynamic conditions to assess the potential of *in situ* remediation treatments. Schnobrich *et al*. (2007) and Haugen (2002) constructed dynamic laboratory experiments simulating groundwater flow through an aquifer and tested the feasibility of using membranes for injection of hydrogen gas as electron donor for autotrophic denitrifying bacteria. Soares *et al.* (1991) studied denitrification in laboratory sand columns inoculated with fresh garden soil and operating at contiunuous and pulse feed regimes. In a different approach, some authors have based their studies on column systems for further application as PRBs. Hunter (2001) and Gibert *et al.* (2008) evaluated the feasibility of using natural materials in PRBs to promote denitrification, specifically the former used vegetable oil and the latter softwood. Furthermore, Moon *et al*. (2008) demonstrated the long-term performance of an autotrophic column system, packed with sulphur granules and limestone, and inoculated with an autotrophic bacterial consortium.

Thus far in the literature, few works applying models to column denitrification studies are found (Schäfer *et al.*, 1998; Zysset *et al.*, 1994). However, several authors have developed mathematical models to describe the fate and transport of nitrate in groundwater systems. Most of these studies, take into account the kinetics and interactions of organic carbon (i.e. substrate) and electron acceptors (i.e. oxygen and nitrate) by using the multiple-Monod kinetics (Killingstad *et al.*, 2002; Kinzelbach *et al.*, 1991; MacQuarrie and Sudicky, 2001; MacQuarrie *et al.*, 2001; Smith *et al.*, 1996; Widdowson *et al.*, 1988). For instance, Widdowson *et al.* (1988) developed a one-dimensional transport model for the biodegradation of organic carbon subject to sequential aerobic and nitrate-based respiration, whereas Killignstad *et al.* (2002) built a two-dimensional numerical transport model to simulate an enhanced *in situ* denitrification experiment performed in a nitrate-contaminated aquifer. Interestingly, the latter added the capability of simulating nitrite transport, production and reduction using a full Monod kinetic model. In a much different approach, Smith *et al.* (1996) studied the intrinsic denitrification of an aquifer by using a zero-order degradation term in a one-dimensional model to describe nitrate reduction.

In recent years, different computer models have been developed for the simulation of transport processes of chemical species involved in biogeochemical reaction processes. For example, Postma *et al.* (1991) successfully used PHREEQM (now available as PHREEQC) to predict the vertical movement of a redoxcline through a sand and gravel aquifer containing pyrite and organic carbon. Furthermore, MODFLOW and RT3D code were used by Wriedt and Rode (2006) and Lee *et al.* (2006) to predict the transport and transformation of nitrate in groundwater.

2. OBJECTIVES

The first objective of this chapter is to study the denitrification process under dynamic conditions by means of a column experiment simulating the flow of groundwater through an aquifer system. The nitrate load and the organic carbon (OC) dosage will be investigated as main factors determining the denitrification potential.

The second objective is to investigate the influence of the bioremediation process on the hydrodynamic characteristics of the column experiment.

The third objective is to develop an integrated model coupling the microbial model built in Chapter 4 with the physical transport processes occurring in the experimental column.

3. MATERIALS AND METHODS

3.1. COLUMN SET-UP

A dynamic experiment was designed to simulate the groundwater flow through an aquifer matrix. The experiment was conducted in a 26 cm long, 2.5 cm inner diameter column constructed of methacrylate and fitted with sampling ports (two-way valve OM-1101, Omnifit) at 6, 14 and 22 cm height. An additional sampling port was installed at the column inlet by using an Omnifit three-way valve single key (OM-1109). A picture and a schematic diagram of the column set-up are provided in Figure 5.1.

The column was filled with a total amount of 271.1 g of homogenized subsoil material sampled in Argentona in January 2009. Soil characteristics are detailed in Chapter 3 (Table 3.4). While packing, the column was gently tapped to achieve homogeneous distribution of the soil. Soil samples for molecular analyses (2 aliquots of 2 g) and dry matter measurement (2 aliquots of approximately 10 g) were collected the same day of the column set-up. Two 2.5 cm diameter discs of fine mesh and glass wool were placed at the bottom and the top of the column to help distribute the flow and prevent the loss of soil particles.

The influent solution was groundwater collected in Argentona during the same sampling campaign of 2009. Chemical groundwater characteristics are provided in Chapter 3 (Table 3.4). Immediately after packing, soil was allowed to equilibrate by continuously pumping groundwater into the column in an upward flow via a peristaltic multi-channel pump (Minipuls 3, Gilson). Electrical conductivity was measured at the outlet of the column by a conductivity cell (No. 52 59, Crison) coupled to a conductivity meter (GLP 32, Crison) until constant value. At this point, it was considered the soil equilibration was completed.

During denitrification tests, the column was fed with a mixture 1:1 of two different influent solutions: a high-nitrate contaminated groundwater and a glucose-amended groundwater. An Omnifit valve (three-way valve, OM-1102), installed immediately before the inlet sampling port, was used to mix both influent solutions. Previous attempts had demonstrated that the mixture of high concentrations of nitrate and glucose in groundwater resulted in an initiation of the denitrification process in the influent solution. Indigenous bacteria from groundwater could reduce nitrate to nitrite and high concentrations of this toxic intermediate were detected before groundwater entered into the column. To avoid this undesirable accumulation of nitrite, two different influent solutions were used in this experiment. These solutions were

frequently prepared by spiking proper amounts of either glucose (Scharlau) or KNO_3 (Scharlau) in groundwater and were stored in sterilized dark bottles to prevent growth of phototrophic bacteria. The column set-up was maintained at dark in a thermostatic chamber at 17°C (Medilow, Selecta) to simulate natural aquifer conditions.

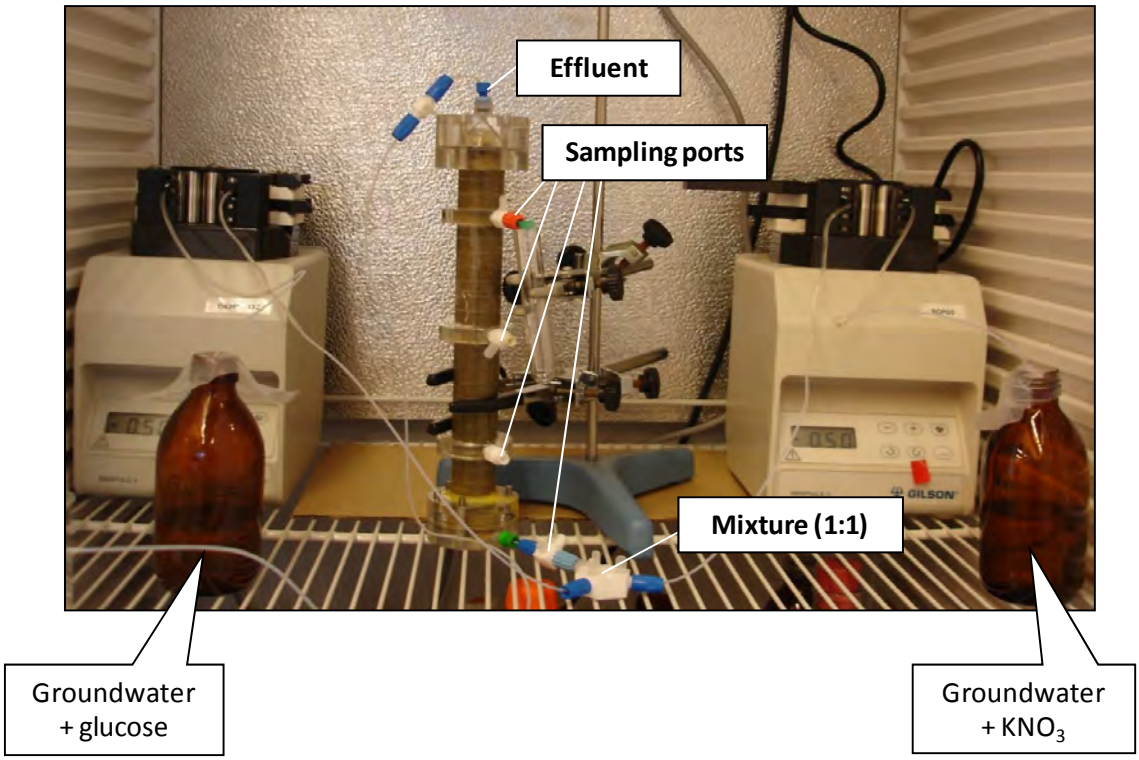

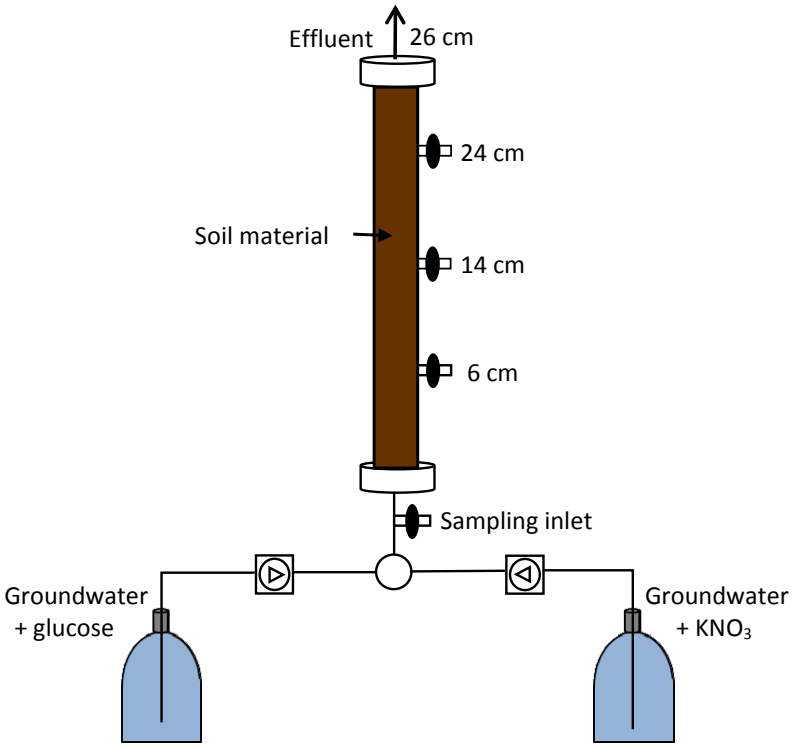

Figure 5.1. Picture (top) and schematic diagram (bottom) of the dynamic experiment operated in this study.

3.2. PHYSICAL AND HYDRAULIC COLUMN CHARACTERISATION

Physical and hydraulic characteristics of the column set-up were determined as follows:

The flow rate (J_W, $L^3 \cdot T^{-1}$) was measured by weighing the water volume corresponding to 60 minutes of pumping and taking into account an ideal density of 1 kg $H_2O \cdot L^{-1}$. The flow rate was determined at the outlet of the Omnifit three-way valve, after the mixture of the two influent solutions (Figure 5.1). In addition, during column operation, the flow rate was routinely checked by weighing the waste reservoir.

The pore volume (V, L^3), the volume of solution inside the column, was calculated by subtracting the weight of the dry soil and column housing from the weight of the fully groundwater saturated column and taking into account the water density.

The dead volume (V_d, L^3) of the experimental system was measured by weighing the water content of all the system tubes (inlet and outlet) and taking into account the water density.

The dead time (t_d, T^{-1}) of the column system was calculated from the J_W and V_d using the following equation:

$$t_d = \frac{V_d}{J_W} \tag{5.1}$$

A first tracer test was carried out to determine the initial hydraulic parameters of the column. A step input of a stock solution of sodium bromide (10^{-5} M) in groundwater was pumped into the equilibrated column at the flow rate of 3 $mL \cdot h^{-1}$ (the same flow rate used in the denitrification tests). Bromide is the most recommended tracer in this type of experiments due to its conservative behaviour in soils and low concentration in natural water (Skaggs *et al.*, 2002); furthermore, it has been widely applied in bioremediation column tests (Moon *et al.*, 2008; Schnobrich *et al.*, 2007; Trudell *et al.*, 1986). Following the same procedure, a second tracer test was performed at the end of the column operation (i.e. after finishing denitrification tests) to determine changes in hydraulic parameters over time.

During the tracer tests, samples were collected from the outlet of the column each 30 min by using a fraction collector (FC203B, Gilson). The midpoint of the sampling interval time was used as the time of the sample. Thus, the time associated to each collected sample was calculated as follows:

$$t_i = \left(\frac{(i \cdot 30)}{60} - 0.25\right) - t_d \qquad \text{(in hours)} \tag{5.2}$$

in which t_i is the time associated to each collected sample (i from 1 to *n* samples).

The hydraulic parameters of the column system were determined by means of the CXTFIT code (Toride *et al.*, 1999) incorporated in the STANMOD program (Simunek *et al.*, 1999). The STANMOD program is useful to obtain the dispersion coefficient (D, $L^2 \cdot T^{-1}$) and the pore water velocity (v_{H2O}, $L \cdot T^{-1}$) of a dynamic system. To calculate these parameters, the program input is the tracer concentration with time in a previously selected position of the column (the outlet in this work). Once these parameters were known, the dispersivity (α, L) and the porosity (ε) in the column were calculated by using the following equations (Appelo and Postma, 2005):

$$\alpha = \frac{D}{v_{H2O}} \tag{5.3}$$

$$\varepsilon = \frac{J_w}{A \cdot v_{H2O}} \tag{5.4}$$

in which A is the cross section area of the column (L^2).

3.3. COLUMN OPERATION AND SAMPLING PROCEDURE

The column operation was divided in five phases, in which different conditions were tested to better assess the denitrification process under dynamic conditions. For an easier comprehension, details of each phase are indicated in Table 5.1. Briefly, in Phase I, groundwater was pumped through the column at a flow rate of 3 $mL \cdot h^{-1}$ for a 26 day period. In subsequent phases, indigenous microorganisms from soil material were stimulated by addition of glucose-amended groundwater (concentration ranging from 150 to 300 $mg \cdot L^{-1}$) while testing different nitrate loads (from 5.0 to 18.1 $mg \cdot L^{-1} \cdot h^{-1}$) either by increasing the influent nitrate concentration (Phases II-IV) or by increasing the flow rate to 5.4 $mL \cdot h^{-1}$ (Phase V).

Periodically, the column was sampled from the top to the bottom to minimize disturbance of the upward flow. Time between samplings was enough to allow at least one change of the pore volume. During sampling, the column outlet was closed and pore water samples were collected from the sampling ports along the column axis (6, 14 and 22 cm). Samples were collected in 10-mL plastic vials by opening the selected Omnifit valve and inserting a fine sterile needle. Enough time to collect a volume about 5 mL samples was waited. Water samples from the inlet and outlet (26 cm) of the column were also collected by the inlet sampling port (OM-1109) and the outlet tube installed in the column, respectively.

Table 5.1. Chronology of the different conditions applied to the experimental column.

Phases	Day	Glucose ($mg \cdot L^{-1}$)[a]	NO_3^- ($mg \cdot L^{-1}$)[a]	Flow rate ($mL \cdot h^{-1}$)	Nitrate load ($mg \cdot L^{-1} \cdot h^{-1}$)[b]	Molar C/N[c]
Phase I	0-26	--	46	3	2.3	--
Phase II	27-39	150	100	3	5.0	3.1
Phase III	40-59	150	150	3	7.5	2.1
Phase IV	60-74	300	200	3	10.0	3.1
Phase V	75-87	300	200	5.4	18.1	3.1

[a] Values correspond to the theoretical influent concentrations.
[b] Calculations were performed taking into account the influent nitrate concentration, the flow rate and the column pore volume (V = 59.8 mL).
[c] C/N: carbon-to-nitrogen molar ratio.

The collected samples were divided in aliquots to analyse nitrate, nitrite and dissolved organic carbon (DOC). Nitrate and nitrite samples were filtered through a 0.22 µm nylon membrane filter and stored at 4°C until analyses, while DOC samples were filtered through a 0.45 µm nylon membrane filter and preserved acidified at -20°C .

Influent and effluent groundwater samples were collected during Phase V (on day 87) for molecular analyses. In addition, after all the phases were completed and the second tracer test was performed (on day 90), soil material for molecular analyses was also collected. Details are indicated in Chapter 6.

3.4. ANALYTICAL METHODS

Nitrate concentration in water samples was determined by High Performance Liquid Chromatography (HPLC, Agilent 2100 series), whereas nitrite concentration was determined by the sulphanilamide colorimetric method using a Shimadzu UV-1603. Both methods are detailed in Chapter 3 (section 3.2.1). DOC was measured by using a Shimadzu TOC 5050 analyzer as described in Chapter 3 (section 3.2.2). Bromide concentrations in water samples from the tracer tests were measured by Inductively Coupled Plasma Mass Spectrometry (ICP-MS, Agilent 7500CX). The water content of soil used in the column was determined after drying the material overnight at 105°C according to the method detailed in Chapter 3 (section 3.3.1).

3.5. MODEL FORMULATION

The mathematical model developed in Chapter 4 describing the aerobic oxidation of organic carbon and denitrification coupled with the heterotrophic microbial growth in batch tests was extended to account for one-dimensional transport. The computer program PHREEQC (Parkhurst and Appelo, 1999) was used to integrate the physical processes of advection and dispersion into the developed model.

Stoichiometric and kinetic parameters used to fulfil the mathematical model were the optimal estimated values obtained in Chapter 4 (section 4.3). The initial hydraulic parameters obtained with the tracer test were used to integrate the transport processes into the model.

4. RESULTS AND DISCUSSION

4.1. COMPARISON OF HYDRODYNAMIC COLUMN CHARACTERISTICS BEFORE AND AFTER APPLYING ENHANCED DENITRIFICATION

In order to investigate whether the denitrification tests had resulted in changes in the hydrodynamic characteristics of the column, a first bromide tracer test was performed before initiating Phase I (once the soil was equilibrated with groundwater), and a second one was done after finishing Phase V. Results of both tracer tests together with the fitted results of the STANMOD program are provided in Figure 5.2.

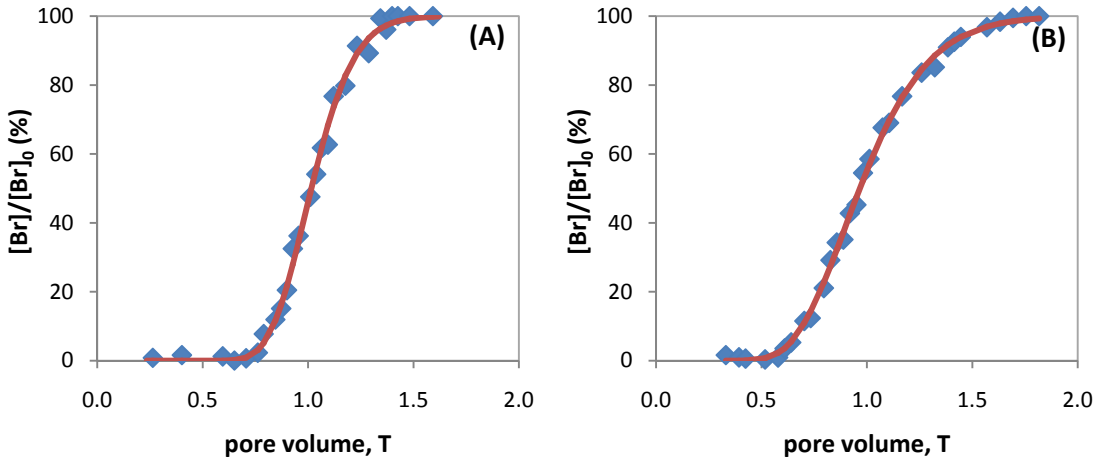

Figure 5.2. Measured bromide effluent breakthrough curves (◆) and fitted models with the CXTFIT code (—) in: (A) before Phase I and (B) after Phase V.

Following the recommendations of Skaggs (2002), breakthrough curves are represented in Figure 5.2 by using dimensionless variables. $[Br]/[Br]_0$ is the ratio of the effluent bromide concentration to the influent concentration and T is a dimensionless time variable that physically corresponds to the number of pore volumes eluted. T was calculated using the following equation:

$$T = \frac{v_{H2O} \cdot t}{L} \tag{5.5}$$

in which t represents the dimensional time variable (T^{-1}) and L de column length (L).

In Figure 5.2 it can easily be observed that an increase of dispersivity occurred inside the column during the application of the denitrification tests. Results of the obtained hydrodynamic parameters are provided in Table 5.2. Before initiating the denitrification tests, the applied flow rate of 3 $mL \cdot h^{-1}$ yielded a pore water velocity of 1.44 $cm \cdot h^{-1}$, and after Phase V the same flow rate yielded a similar pore water velocity of 1.61 $cm \cdot h^{-1}$. Therefore, the hydraulic retention time (HRT) in the column slightly decreased from initial 0.75 d to 0.67 d at the end. However, main differences were observed in the hydrodynamic dispersion coefficient and the porosity of the system. The dispersion coefficient increased from initial 0.48 $cm^2 \cdot h^{-1}$ to 1.5 $cm^2 \cdot h^{-1}$ at the end, which, in turn, resulted in an increase of the dispersivity from 0.33 cm to 0.90 cm. Concerning the effective porosity, the slight increase in pore water velocity resulted in a decrease of the calculated porosity from 42% to 38%.

Similar changes in hydrodynamic properties after applying bioremediation treatments have been reported in literature (Moon *et al.*, 2008; Soares *et al.*, 1991; Taylor and Jaffe, 1990). Taylor and Jaffe (1990) related the increase of dispersivity in a porous media to a biofilm growth, whereas Soares *et al.* (1991) concluded that in sand denitrification columns the increase of dispersivity and pore water velocity was mainly due to the accumulation of gas inside the columns.

Table 5.2. Hydrodynamic parameters before and after denitrification tests.

Parameters	Before tests	After tests
Pore water velocity (v_{H2O})($cm \cdot h^{-1}$)	1.44 ± 0.01	1.61 ± 0.01
Hydraulic retention time (HRT) (d)[a]	0.75 ± 0.01	0.67 ± 0.01
Dispersion coefficient (D) ($cm^2 \cdot h^{-1}$)	0.48 ± 0.07	1.5 ± 0.1
Dispersivity (α) (cm)	0.33 ± 0.05	0.90 ± 0.07
Effective porosity (ε) (%)	42.4 ± 0.4	38.0 ± 0.4

[a] Calculations were performed taking into account the column length (26 cm).

As indicated in Table 5.2, the initial pore water velocity was 1.44 cm·h^{-1} (0.35 m·d^{-1}). This water velocity is in the range of the estimated water velocity in Argentona aquifer. According to Darcy's law the water velocity in Argentona aquifer was calculated as:

$$v_{H2O} = \frac{K \cdot \Delta h/\Delta x}{\varepsilon} \quad (5.6)$$

where K is the hydraulic conductivity (L·T^{-1}) and $\Delta h/\Delta x$ is the hydraulic gradient. As detailed in Chapter 3 (section 3.1), in the studied site the hydraulic conductivity was estimated to be between 5 and 20 m·day^{-1}, the hydraulic gradient was measured to be ~0.0125 m·m^{-1} and the porosity was estimated to be in the interval between 15 and 25% (Grandia *et al.*, 2007). Therefore, according to equation 5.6, a water velocity from 0.25 to 1.67 m·day^{-1} may be expected in the studied site.

4.2. EVALUATION OF THE DENITRIFICATION PROCESS UNDER DYNAMIC CONDITIONS

The constructed column operated with an advective flow, simulating the groundwater seep through an aquifer. As previously mentioned, five different influent conditions were applied, in which a gradual increase of the nitrate load was tested (Phases II-V). In addition, the intrinsic denitrification potential of the aquifer material (Phase I) and the influence of the C/N ratio pumped into the column (Phases II-III) were also investigated.

The column was maintained under natural conditions for a period of 26 days (Phase I), in which groundwater was pumped into the column at the flow rate of 3 mL·h^{-1} (Table 5.1). Samples for nitrate, nitrite and DOC measurement were regularly collected within this period and results demonstrated that no denitrification took place along the column. In addition, DOC in collected pore water samples was always below or close to the detection limit (1 mg·L^{-1}) (data not shown), corroborating the low OC availability in the system. These results were in agreement with previous microcosm tests (Chapter 3, section 4.2.1), and corroborated that an amendment with an electron donor was required to promote denitrification in the aquifer material.

After 26 days running under natural conditions, column influent was changed for high-nitrate contaminated groundwater amended with glucose (Phase II). Glucose and nitrate were added to groundwater in a C/N molar ratio of 3.1, which corresponded to a value slightly higher than the theoretical calculated C/N ratio of 2.7 (Chapter 3, section 4.3), since it was taken into

account that the influent groundwater was aerobic (about 9 $mg \cdot L^{-1}$ dissolved oxygen). Results demonstrated a high denitrification potential in the column when amending the influent with an organic substrate (Figure 5.3). After 5 days of continuously feeding the column with glucose (32nd day of total operation), complete nitrate removal was demonstrated in the first sampling port (6 cm) of the column (Figure 5.3A). However, nitrite concentration reached a maximum of 6.4 $mg \cdot L^{-1}$ at 6 cm, which could not be completely reduced along the height of the column (effluent concentration was 2.1 $mg \cdot L^{-1}$). Concerning organic carbon, a DOC removal of about 75% was measured in the first 6 cm of the column, increasing to a removal higher than 95% at the column effluent. Subsequent samplings demonstrated that accumulated nitrite could be completely reduced along the height of the column (Figure 5.3B) and after 9 days of column operation under conditions of Phase II (36th day of total operation), complete nitrate and nitrite removal was observed within the first 6 cm of the column (data not shown). The transient nitrite accumulation observed on first days of Phase II operation corroborates a time lag between the onset of nitrate reduction and the subsequent onset of nitrite reduction, as observed in previous microcosm tests (Chapter 3).

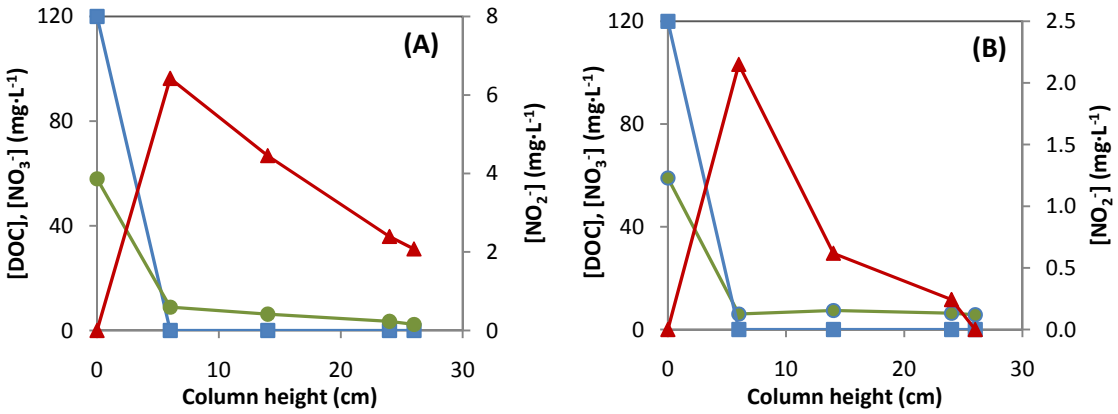

Figure 5.3. Nitrate (■), nitrite (▲) and DOC (●) profiles obtained along the height of the column on the 5th day (A) and the 7th day (B) of column operation under a nitrate load = 5.0 $mg \cdot L^{-1} \cdot h^{-1}$ and a C/N molar ratio = 3.1 (Phase II).

Overall, results pointed to the fact that the continuous feed of the column with glucose resulted in a biomass population growth in the first centimetres of the column, which was able to consume all the available glucose and nitrate from influent solution. A rather important result is that the obtained data indicates that a non desirable accumulation of nitrite may happen in early stages of bioremediation treatment applications.

In order to investigate denitrification in carbon limited conditions, Phase III was started on day 40 by pumping into the column groundwater spiked with an excess of nitrate (C/N molar ratio

of 2.1). This excess of nitrogen was achieved by increasing the influent nitrate concentration to 150 mg·L^{-1}. Results obtained during this phase demonstrated that nitrate and DOC were completely removed within the column (Figure 5.4). However, produced nitrite could not be further reduced and more than 25 mg·L^{-1} (22% of influent nitrate concentration) of this toxic intermediate was detected in the column effluent. Again, it was observed that main processes occurred within the first 6 cm of the column. On average, about 95% and 85% of influent nitrate and DOC concentrations, respectively, were removed before the first sampling port. Moreover, the accumulation of nitrite observed at 6 cm was maintained constant until the outlet of the column (Figure 5.4).

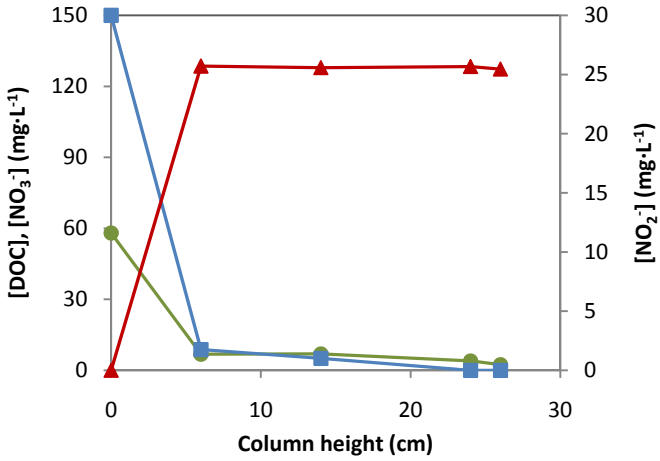

Figure 5.4. Nitrate (■), nitrite (▲) and DOC (●) profiles obtained along the height of the column under a nitrate load = 7.5 mg·L^{-1}·h^{-1} and C/N molar ratio = 2.1 in steady-state conditions (Phase III).

Although the column was operated for 19 days at the reduced C/N ratio, the profiles of nitrate, nitrite and DOC were quite stable over time. Nitrite began to accumulate immediately after amending the influent with an excess of nitrate, and after 2 days of operation, steady-state conditions for the consumption of nitrate and accumulation of nitrite were reached inside the column.

Overall, results obtained in this phase demonstrated that a lack of glucose resulted in a complete removal of nitrate inside the column, although an average of 22% of the influent nitrate concentration was accumulated as nitrite. This finding agree with the previous results obtained in microcosm tests (Chapter 3), where the accumulation of nitrite was suggested to be related with a lack of substrate due to aerobic respiration. Furthermore, similar results were reported by Oh and Silverstein (1999) in a denitrifying activated sludge mixed liquor when the addition of acetate as electron donor was limited. Almeida *et al*. (1995) investigated the competition between nitrate and nitrite reduction using *Pseudomonas fluorescens* and

suggested that nitrate and nitrite reductases (i.e. the enzymes responsible of nitrate and nitrite reduction) compete for the oxidation of common electron donors. Therefore, it is suggested that a competition between both enzymes for the electrons generated by the oxidation of glucose was the main process causing the accumulation of nitrite inside the column.

In Phase IV, glucose and nitrate concentrations were increased to achieve again a C/N ratio of 3.1 in the influent groundwater. However, the nitrate load applied to the column in this phase was increased to 10.0 $mg \cdot L^{-1} \cdot h^{-1}$. Interestingly, similar results to Phase I were obtained, corroborating that the denitrification process in the aquifer material was mainly controlled by the electron donor availability. Nitrate and nitrite reduction together with a decrease in DOC were observed in the first 6 cm of the experimental column (data not shown).

It is important to note that, after the C/N ratio was restored to 3.1, the system reached the steady-state more rapidly than in Phase I, indicating the adaptability of the microbial population to denitrify. After two days of operating in this stage, a peak of only 0.6 $mg \cdot L^{-1}$ of nitrite was observed at 6 cm which could be completely reduced before the second sampling port at 14 cm. Subsequent sampling campaigns showed complete nitrate and nitrite removal at 6 cm height. Therefore, the complete denitrification was attained in the first layers of the soil column, demonstrating that the maximum system capacity was higher than the tested nitrate loads.

On day 75 of column operation, the flow rate of the influent was increased to 5.4 $mL \cdot h^{-1}$ (Phase V), whereas glucose and nitrate were supplied to the column in the same concentrations as in Phase IV. This resulted in an increase of the nitrate load to 18.1 $mg \cdot L^{-1} \cdot h^{-1}$. Results indicated that a higher length to achieve complete denitrification inside the column was needed under these conditions (Figure 5.5). A total removal of 88% of nitrate and 78% of DOC was observed within the first 6 cm in steady-state conditions for the studied species. Nitrite was detected in the first sampling port, but its concentration accounted for less than 3% of the influent nitrate concentration. However, the total length of the column was still sufficient to attain complete nitrate and nitrite reduction and to ensure good quality, in terms of nitrogen species and DOC of the effluent water.

In conclusion, under the dynamic conditions assayed results indicated that aerobic and denitrifying bacteria were developed exclusively in the first centimetres of the column, where they could consume all the available nitrate and oxygen content of the influent solution.

Growth of facultative heterotrophs in the first layers of column experiments were also reported in other studies (Soares *et al.*, 1991; Von Gunten and Zobrist, 1993). For instance, Von Gunten and Zobrist (1993) observed that the group of aerobic and denitrifying bacteria developed exclusively in the first centimetre of an experimental column filled with river sediments and continuously fed with synthetic river water containing lactate and electron acceptors (6.1 $mg \cdot L^{-1}$ oxygen and 18.6 $mg \cdot L^{-1}$ nitrate among others) and operating at a constant pore water velocity of 0.94 $m \cdot d^{-1}$. An additional result from these tests is that the assayed system was appropriate to denitrify high nitrate loads (up to 18 $mg \cdot L^{-1} \cdot h^{-1}$). Furthermore, as mentioned above, the maximum capacity of the system was not achieved in this study, indicating the potential of organic substrate injection for *in situ* groundwater denitrification.

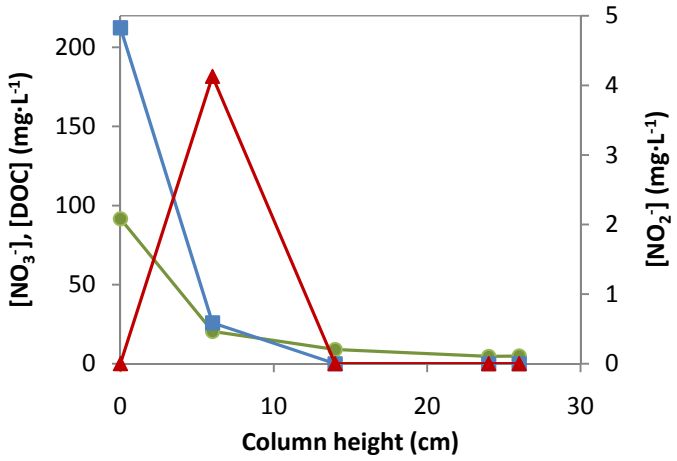

Figure 5.5. Nitrate (■), nitrite (▲) and DOC (●) profiles obtained along the height of the column under a nitrate load = 18.1 $mg \cdot L^{-1} \cdot h^{-1}$ and C/N molar ratio = 3.1 in steady-state conditions (Phase V).

4.3. MODELLING DENITRIFICATION IN A SATURATED POROUS MEDIA: APPLICATION TO THE DYNAMIC EXPERIMENT

A mathematical model to predict the transport and fate of nitrate, dissolved oxygen (DO) and organic carbon in the experimental column is presented in this section. The model is based on the enhanced denitrification model presented in Chapter 4, which describes the aerobic oxidation of organic matter and denitrification coupled with the growth and decay of a facultative heterotrophic microbial population in a batch experimental system. As previously mentioned, the optimal parameters estimated in Chapter 4 were used in simulations. PHREEQC was used to model a one-dimensional (1D) flow path of groundwater through the experimental column. Discretization of the column and physical and hydraulic parameters used in simulations are detailed in Table 5.3.

Table 5.3. Physical and hydraulic parameters and column discretization used for simulations.

Property	Value	Units
Physical or hydraulic parameter		
Column length (L)	26	cm
Effective porosity (ε)[a]	42	%
Bulk density[b]	1.45	kg·L^{-1}
Pore water velocity (v_{H2O})[a]	1.44	cm· h^{-1}
Dispersion coefficient (D)[a]	0.48	cm^2·h^{-1}
Longitudinal dispersivity (α)[a]	0.33	cm
Discretization		
Spatial discretization	50 cells	
Temporal discretization[c]	646 steps of 0.37 h step length	

[a] Parameters calculated by means of the bromide tracer test and the CXTFIT code before Phase I.
[b] Calculation was performed by taking into account the mass of dry soil in the column and the total volume of the column.
[c] Correspond to a simulation time of 10 days.

As indicated in Table 5.3, the column was represented in the 1D model by a grid of 50 cells, each having a length of 0.52 cm. This spatial discretization was sought to give a grid-Peclet number smaller than 2 to avoid numerical error of physical transport (Kinzelbach *et al.*, 1991). The grid-Peclet number (Pe) is related to the cell length (Δx) and is defined as:

$$Pe = \frac{v_{H2O} \cdot \Delta x}{D} \tag{5.7}$$

Based on the pore water velocity and the dispersion coefficient of 1.44 cm·h^{-1} and 0.48 cm^2·h^{-1}, respectively, Pe in the model was calculated to be 1.6.

Moreover, to limit the effects of numerical dispersion, temporal discretization was calculated considering that Courant number should be approximately 1 (Kinzelbach *et al.*, 1991). The Courant number (Cr) is related to the time step (Δt) and is calculated by using the following expression:

$$Cr = \frac{v_{H2O} \cdot \Delta t}{\Delta x} \tag{5.8}$$

The model simulated a step addition of nitrate-contaminated groundwater amended with glucose into the soil column during 10 days. Prior to this step solution injection, the column was considered to be filled with groundwater. Therefore, the background concentration was 50 mg·L^{-1} of nitrate and 9 mg·L^{-1} of DO, with no availability of organic carbon. pH and pe were considered to be 7 both in the background solution and the step solution, which approximately

correspond to pH and pe values measured in groundwater (Chapter 3, Table 3.4). The step solution was the influent solution pumped into the column during Phase II, therefore, it was considered to contain 150 mg·L^{-1} of glucose, 100 mg·L^{-1} of nitrate and 9 mg·L^{-1} of DO.

First simulation results showed a high growth of heterotrophic bacteria immediately at the column inlet, where the constant organic carbon supply allowed the modelled microorganisms to consume all available oxygen and nitrate. After 5 days of column feeding, simulated concentrations at 0.26 cm height were 2.4 mg·L^{-1} nitrate and negligible DO and glucose concentrations. Regarding the biomass population, the model predicted a concentration up to 8 g·L^{-1} at the same height.

Intuitively, in a porous medium there will be physical and hydrodynamic constraints on the maximum biomass concentration. To account for these limitations, some authors have used the maximum microbial capacity concept, based on the following formulation proposed by Kindred and Celia (1989):

$$F(X) = \frac{K_b}{K_b + X} \tag{5.9}$$

in which $F(X)$ refers to the biomass inhibition term, X is the concentration of biomass (M·L^{-3}) and K_b is the biomass inhibition coefficient (M·L^{-3}). The concept refers to the fact that net microbial growth is reduced when the population of bacteria approaches a threshold value. The use of this inhibition term in the microbial kinetics considered in Chapter 4 (Table 4.5) prevented excessive microbial growth at the immediate column inlet in the model and forced the microorganisms to extend their activities along the column.

Relatively few studies applying the maximum microbial capacity concept were found in literature. Furthermore, there is no general agreement on a K_b value for bacteria growing in soils, and values ranging from 0.5 mg·L^{-1} to 1.6 g·L^{-1} have been reported in literature (Kindred and Celia, 1989; Lee *et al.*, 2006; MacQuarrie and Sudicky, 2001; Schäfer *et al.*, 1998; Zysset *et al.*, 1994). To be consistent, this value should be calibrated with specific experiments. However, the performed dynamic experiment did not allow such parameter calibration, since all the biological processes were completed before the first sampling port and no profiles of nitrate and DOC concentrations could be obtained along the height of the column. Nevertheless, different values within the mentioned range were tested in the model. Results demonstrated that, when using K_b<0.2 g·L^{-1}, simulated nitrate had concentrations higher than 10 mg·L^{-1} at 6 cm height of the column, whereas when using K_b = 1.6 g·L^{-1} denitrification was almost completed within the first 2 cm of the aquifer column (simulated nitrate concentration

lower than 5 mg·L^{-1}). The biomass concentration went up to 0.7 and 3.7 g·L^{-1} at 0.26 cm height with K_b values of 0.2 and 1.6 g·L^{-1}, respectively. It is important to note that all these results are in steady-state conditions for the measured variables (after 5 days of column feeding). Therefore, taking into account the experimental results obtained during Phase II of column operation, a K_b value between 0.2 g·L^{-1} and 1.6 g·L^{-1} seemed reasonably. Overall, it was observed that K_b had a great influence on the simulation results and thus more experiments would be needed to calibrate properly this parameter.

In Figure 5.6 simulated nitrate and DOC profiles along the height of the column when considering a K_b value of 1.2 g·L^{-1} as proposed by Zysset *et al.* (1994) are presented. It can be observed that the simulated nitrate concentration dropped in the first centimetres of the column, although remained at a residual concentration of less than 3 mg·L^{-1}. However, this residual concentration of nitrate may be considered negligible if it is taken into account that constitutes a value lower than the detection limit of the method applied to measure nitrate in pore water samples.

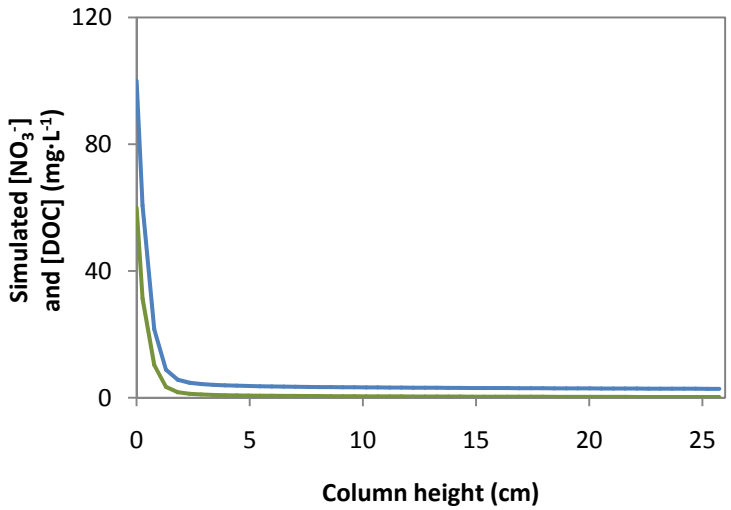

Figure 5.6. Model-predicted concentrations of nitrate (—) and DOC (—) after 5 days of column feeding (steady-state conditions).

As mentioned above, the model predicted steady-state conditions after 5 days of column feeding with glucose and nitrate. However, experimental results demonstrated that more than 5 days were needed to achieve steady-state conditions in Phase II of column operation. It is suggested that in experimental conditions the steady-state was achieved later in Phase II due to the microbial acclimation period, which is not taken into account in the model.

The model was extended to explain denitrification as a two step reaction: nitrate reduction to nitrite and nitrite reduction to nitrogen gas. Relatively few studies have integrated the

production and subsequent reduction of nitrite as an intermediate of the denitrification process in models (Almeida *et al.*, 1995; Killingstad *et al.*, 2002; Smith *et al.*, 2001; Vasiliadou *et al.*, 2006), and most of them have used the non-competitive model. The non-competitive model considers that nitrate is preferentially used as an electron acceptor by microorganisms due to a higher energy yield relative to nitrite. It can be mathematically expressed by the following hyperbolic function, which has the same general form as equation 5.9 (Soto *et al.*, 2007):

$$F(NO_2^-) = \frac{K_{NO3,I}}{NO_3^- + K_{NO3,I}} \tag{5.10}$$

in which $F(NO_2^-)$ refers to the nitrite non-competitive inhibition term, $K_{NO3,I}$ is the inhibition coefficient for nitrate (M·L^{-3}) and NO_3^- is the nitrate concentration (M·L^{-3}). There are other types of kinetic relationships that could be used instead of equation 5.10. For example, Vasiliadou *et al.* (2006) proposed a model which treated nitrate and nitrite as substitutable substrates to describe hydrogenotrophic denitrification in batch assays. However, the reasons to select the non-competitive model in this project were based on the experimental results, which demonstrated an accumulation of nitrite while nitrate was completely removed, together with the fact that this model appeared to be one of the most commonly applied in literature. In this way, the specific growth rate (μ) for nitrite-based respiration was expressed as:

$$\mu = \mu_{max,H} \cdot \frac{OC}{OC + K_{OC}} \cdot \frac{NO_2^-}{NO_2^- + K_{NO2}} \cdot \frac{K_{NO3,I}}{NO_3^- + K_{NO3,I}} \cdot \frac{K_b}{X_H + K_b} \cdot \eta \tag{5.11}$$

According to Smith *et al.* (2001) a $K_{NO3,I}$ value of 8.68 mg nitrate·L^{-1} was used in simulations. In addition, the saturation coefficient for nitrite (K_{NO2}) was considered to have the same value as the saturation coefficient for nitrate (K_{NO3}) in molar units (i.e. 1.64 mg·L^{-1} nitrite) (Smith *et al.*, 2001). All the other kinetic parameters are detailed in Chapter 4 (section 4.3).

Stoichiometric reactions considering nitrate reduction to nitrite and subsequent nitrite reduction to nitrogen gas were developed taking into account an f_s value of 0.67 (Henze *et al.*, 2000):

$$0.042C_6H_{12}O_{6(aq)} + 0.189NO^-_{3(aq)} + 0.024H^+_{(aq)} \rightarrow$$
$$0.165NO^-_{2(aq)} + 0.024C_5H_7O_2N_{(cell)} + 0.130\ CO_{2(g)} + 0.178\ H_2O \tag{5.12}$$

$$0.042C_6H_{12}O_{6(aq)} + 0.136NO^-_{2(aq)} + 0.136H^+_{(aq)} \rightarrow$$
$$0.055N_{2(g)} + 0.026C_5H_7O_2N_{(cell)} + 0.121\ CO_{2(g)} + 0.227H_2O \tag{5.13}$$

The stoichiometric C/N molar ratios were calculated to be 1.3 for nitrate reduction to nitrite (equation 5.12) and 1.8 for nitrite reduction to nitrogen gas (equation 5.13). These values were integrated into the model to explain nitrite production and subsequent reduction.

Again, the model was run with the experimental conditions from Phase II. Results predicted a complete removal of nitrate but an accumulation of the intermediate nitrite (about 21 $mg \cdot L^{-1}$) inside the column, which could not be further reduced (data not shown). However, as previously mentioned, in the column test complete nitrate and nitrite removal were attained within the Phase II of column operation. Differences between the experimental results and model simulations were observed to be mainly due to the considered stoichiometric ratios. As indicated in Chapter 4, mainly two reasons could explain these discrepancies. On the one hand, the model is based on the theoretical development of microbial reactions and, therefore, may only be considered as an approach to explain these processes. On the other hand, in the soil column, the presence of other organic substrates besides glucose may be used by microorganisms increasing the denitrification potential.

When increasing the input glucose concentration in the model, complete nitrate and nitrite removals were predicted. Specifically, an increase of 20% of the influent glucose concentration was tested and results demonstrated the complete denitrification before 6 cm height. Simulated concentrations in transient conditions and steady-state in the first 10 cm of the column are shown in Figure 5.7. The model predicted an accumulation of nitrite inside the column which could not be completely reduced during the first hours of the test (Figure 5.7A). This finding agrees with the experimental results obtained during the first days of column operation under the conditions of Phase II (Figure 5.3A), demonstrating that the non-competitive model could be used for explaining the nitrite accumulation in the first stages of a bioremediation nitrate treatment. However, the time required to achieve steady-state in the model prediction and the experiment was different again, which could be due to the fact that the model did not take into account the microbial acclimation period. Furthermore, the high predicted transient accumulation of nitrite (up to 55 $mg \cdot L^{-1}$ at 6 cm height) is due to the use of a low inhibition coefficient $K_{NO3,I}$. Again, the calibration of this parameter should be performed to explain properly the accumulation of nitrite under specific experimental circumstances. In steady-state conditions, the model predicted complete denitrification within the first 6 cm of the column, although high accumulation of nitrite, up to 35 $mg \cdot L^{-1}$ at 0.26 cm height, was observed (Figure 5.7B).

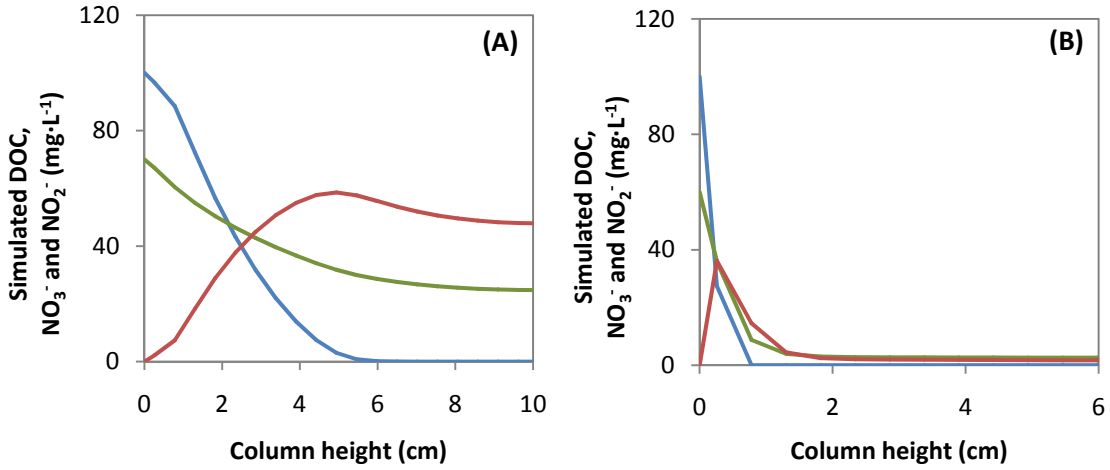

Figure 5.7. Model-predicted concentrations of nitrate (—), DOC (—) and nitrite (—) in: (A) transient conditions (after 37 hours of column operation) and (B) steady-state conditions (5th day column operation).

Overall, the mathematical model developed herein was intended to be an approach to describe the transformations and transport of nitrate and DOC in a dynamic denitrification experiment simulating the seep of groundwater through an aquifer. Calibration and validation of the model could not be done by means of the performed experiment. Nevertheless, the model could explain the growth of heterotrophic bacteria in the immediately inlet of the column. In addition, the extension of the model to explain denitrification as a two step process could describe the initial accumulation of nitrite and subsequent reduction inside the column. However, much work should be done, first, in calibrating the most outstanding parameters when considering the denitrification as a two step process (e.g. following the model development described in Chapter 4) and, second, in performing specific-designed dynamic experiments to validate the developed model under these conditions.

5. CONCLUSIONS

A dynamic experiment performed in a soil column fed with groundwater corroborated that aquifer material could not trigger denitrification without the addition of an electron donor.

The addition of glucose to the influent groundwater promoted denitrification within the first soil layers of the column. A nitrate load up to 18 mg·L^{-1}·h^{-1} could be successfully removed from groundwater in the experimental system.

A transient nitrite accumulation along the height of the column, resulting from nitrate reduction, was observed during the first days of bioremediation tests. In addition, the supply

of glucose-limited groundwater to the column resulted in a high and persistent accumulation of nitrite, whereas nitrate was completely reduced.

The nitrate load was demonstrated to be related to the column length needed to complete the denitrification process. However, the system maximum capacity was not attained with the studied experimental conditions and denitrification was always completed within the height of the column.

Hydrodynamic parameters in the column experimented changes after applying the enhanced denitrification tests. Specially, dispersivity increased and effective porosity decreased. Similar results are reported in literature in bioremediation dynamic experiments. It is suggested that these changes may be due to the growth of biomass or the accumulation of gas inside the column.

A model coupling the microbial mediated reactions with the transport processes occurring inside the column was implemented by means of PHREEQC. The maximum microbial capacity concept seemed to be a crucial parameter to account for the effect of limited pore space.

Nitrite as intermediate in the denitrification process was integrated in the dynamic model considering the non-competitive inhibition kinetics. Results could predict the transient accumulation of nitrite inside the column in first stages of enhanced denitrification. However, since the model did not take into account the microbial acclimation period, predicted steady-state conditions were attained more rapidly than the observed experimental results.

Calibration of kinetic parameters should be performed to adjust properly the model to experimental results. However, the performed experiment could not be used for such calibration.

6. REFERENCES

Almeida, J.S., Reis, M.A.M. and Carrondo, M.J.T. 1995. Competition between nitrate and nitrite reduction in denitrification by *Pseudomonas fluorescens*. *Biotechnology and Bioengineering*, 46, 476-484.

Appelo, C.A.J. and Postma, D. 2005. Geochemistry, groundwater and pollution. A.A. Balkema Publishers. Amsterdam, The Netherlands.

Beller, H.R., Madrid, V., Hudson, G.B., McNab, W.W. and Carlsen, T. 2004. Biogeochemistry and natural attenuation of nitrate in groundwater at an explosives test facility. *Applied Geochemistry*, 19, 1483-1494.

Gibert, O., Pomierny, S., Rowe, I. and Kalin, R.M. 2008. Selection of organic substrates as potential reactive materials for use in a denitrification permeable reactive barrier (PRB). *Bioresource Technology*, 99(16), 7587-7596.

Grandia, F., Domènech, C., Jordana, S., Goscera, G., Arcos, D., Duro, L., Guimerà, J. and Bruno, J. 2007. Reactive transport modelling of denitrification plumes induced by organic matter injection. In: *Proceedings of the water pollution in natural porous media at different scales. Assessment of fate, impact and indicators. WAPO*^{2}*.* Barcelona (Spain).

Haugen, K.S., Semmens, M. J. and Novak, P. J. 2002. A novel in situ technology for the treatment of nitrate contaminated groundwater. *Water Research*, 36, 3497-3506.

Henze, M., Gujer, W., Mino, T. and van Loosdrecht, M. 2000. Activated sludge models ASM1, ASM2, ASM2D and ASM3. Scientific and technical report no.9. London: IWA Publishing.

Hunter, W.J. 2001. Use of vegetable oil in a pilot-scale denitrifying barrier. *Journal of Contaminant Hydrology*, 53, 119-131.

Khan, I.A. and Spalding, R.F. 2003. Development of a procedure for sustainable in situ aquifer denitrification. *Remediation Journal*, 13, 53-69.

Khan, I.A. and Spalding, R.F. 2004. Enhanced in situ denitrification for a municipal well. *Water Research*, 38, 3382-3388.

Killingstad, M.W., Widdowson, M.A. and Smith, R.L. 2002. Modeling enhanced in situ denitrification in groundwater. *Journal of Environmental Engineering*, 128, 491-504.

Kindred, J.S. and Celia, M.A. 1989. Contaminant transport and biodegradation. 2. conceptual-model and test simulations. *Water Resources Research*, 25, 1149-1159.

Kinzelbach, W., Schafer, W. and Herzer, J. 1991. Numerical modeling of natural and enhanced denitrification processes in aquifers. *Water Resources Research*, 27, 1123-1135.

Lee, M.S., Lee, K.K., Hyun, Y.J., Clement, T.P. and Hamilton, D. 2006. Nitrogen transformation and transport modeling in groundwater aquifers. *Ecological Modelling*, 192, 143-159.

Lensing, H.J., Vogt, M. and Herrling, B. 1994. Modeling of biologically mediated redox processes in the subsurface. *Journal of Hydrology*, 159, 125-143.

MacQuarrie, K.T.B. and Sudicky, E.A. 2001. Multicomponent simulation of wastewater-derived nitrogen and carbon in shallow unconfined aquifers I. Model formulation and performance. *Journal of Contaminant Hydrology*, 47, 53-84.

MacQuarrie, K.T.B., Sudicky, E.A. and Robertson, W.D. 2001. Multicomponent simulation of wastewater-derived nitrogen and carbon in shallow unconfined aquifers II. Model application to a field site. *Journal of Contaminant Hydrology*, 47, 85-104.

Moon, H.S., Shin, D.Y., Nam, K. and Kim, J.Y. 2008. A long-term performance test on an autotrophic denitrification column for application as a permeable reactive barrier. *Chemosphere*, 73, 723-728.

NITRABAR. 2009. A novel tool to assist in the reduction of agricultural diffuse nitrate pollution in Europe. (http://nitrabar.eu).

Oh, J. and Silverstein, J. 1999. Acetate limitation and nitrite accumulation during denitrification. *Journal of Environmental Engineering-Asce*, 125, 234-242.

Parkhurst, D.L. and Appelo, C.A.J. 1999. User's guide to PHREEQC (version 2). A computer program for speciation, batch-reaction, one-dimensional transport and inverse geochemical calculations, Denver, Colorado.

Postma, D., Boesen, C., Kristiansen, H. and Larsen, F. 1991. Nitrate reduction in an unconfined sandy aquifer - water chemistry, reduction processes and geochemical modeling. *Water Resources Research*, 27, 2027-2045.

Robertson, W.D., Blowes, D.W., Ptacek, C.J. and Cherry, J.A. 2000. Long-term performance of in situ reactive barriers for nitrate remediation. *Ground Water*, 38, 689-695.

Schäfer, D., Schäfer, W. and Kinzelbach, W. 1998. Simulation of reactive processes related to biodegradation in aquifers - 2. Model application to a column study on organic carbon degradation. *Journal of Contaminant Hydrology*, 31, 187-209.

Schipper, L.A., Barkle, G.F., Hadfield, J.C., Vojvodic-Vukovic, M. and Burgess, C.P. 2004. Hydraulic constraints on the performance of a groundwater denitrification wall for nitrate removal from shallow groundwater. *Journal of Contaminant Hydrology*, 69, 263-279.

Schnobrich, M.R., Chaplin, B.P., Semmens, M.J. and Novak, P.J. 2007. Stimulating hydrogenotrophic denitrification in simulated groundwater containing high dissolved oxygen and nitrate concentrations. *Water Research*, 41, 1869-1876.

Simunek, J.M., van Genuchten, T., Sejna, M., Toride, N. and Leij, F.J. 1999. The STANMOD computer software for evaluating solute transport in porous media using analytical solutions of convection-dispersion equation, US Salinity Laboratory Agricultural Research Service: Riverside, California.

Skaggs, T.H., Wilson, G.V., Shouse, P.J. and Leij, F.J. 2002. Solute Transport: Experimental Methods. In: Dane, J.H. and Topp C. (ed.) Methods of Soil Analysis. Part 4-Physiscal Methods. Soil Science Society of America, Inc. Wisconsin, USA. pp. 1381-1402.

Smith, R.L., Garabedian, S.P. and Brooks, M.H. 1996. Comparison of denitrification activity measurements in groundwater using cores and natural-gradient tracer tests. *Environmental Science & Technology*, 30, 3448-3456.

Smith, R.L., Miller, D.N., Brooks, M.H., Widdowson, M.A. and Killingstad, M.W. 2001. In situ stimulation of groundwater denitrification with formate to remediate nitrate contamination. *Environmental Science & Technology*, 35, 196-203.

Soares, M.I.M., Braester, C., Belkin, S. and Abeliovich, A. 1991. Denitrification in laboratory sand columns - carbon regime, gas accumulation and hydraulic-properties. *Water Research*, 25, 325-332.

Soto, O., Aspe, E. and Roeckel, M. 2007. Kinetics of cross-inhibited denitrification of a high load wastewater. *Enzyme and Microbial Technology*, 40, 1627-1634.

Taylor, S.W. and Jaffe, P.R. 1990. Biofilm growth and the related changes in the physical-properties of a porous medium. 3. dispersivity and model verification. *Water Resources Research*, 26, 2171-2180.

Toride, N., Leij, F.J. and v. Genuchten, M.T. 1999. The CXTFIT code for estimating transport parameters from laboratory or field tracer experiments, US Salinity Laboratory Agricultural Research Service: Riverside, California.

Trudell, M.R., Gillham, R.W. and Cherry, J.A. 1986. An in situ study of the occurrence and rate of denitrification in a shallow unconfined sand aquifer. *Journal of Hydrology*, 83, 251-268.

Vasiliadou, I.A., Pavlou, S. and Vayenas, D.V. 2006. A kinetic study of hydrogenotrophic denitrification. *Process Biochemistry*, 41, 1401-1408.

von Gunten, U. and Zobrist, J. 1993. Biogeochemical changes in groundwater-infiltration systems: column studies. *Geochimica Et Cosmochimica Acta*, 57, 3895-3906.

Widdowson, M.A., Molz, F.J. and Benefield, L.D. 1988. A numerical transport model for oxygen-based and nitrate-based respiration linked to substrate and nutrient availability in porous-media. *Water Resources Research*, 24, 1553-1565.

Wriedt, G. and Rode, M. 2006. Modelling nitrate transport and turnover in a lowland catchment system. *Journal of Hydrology*, 328, 157-176.

Zhao, L., Yang, Y.S., Tan, X. and Kalin, R.M. 2003. Removal of nitrate contaminant in porous media aquifer through microbiological method. *Bulletin of Environmental Contamination and Toxicology*, 71, 362-369.

Zysset, A., Stauffer, F. and Dracos, T. 1994. Modeling of reactive groundwater transport governed by biodegradation. *Water Resources Research*, 30, 2423-2434.

PART I - Chapter 6

MOLECULAR TECHNIQUES APPLIED TO THE STUDY OF DENITRIFIERS IN ENHANCED DENITRIFICATION PROCESSES

1. INTRODUCTION

Over the past decade, the use of molecular methods targeting the ribosomal gene 16S rRNA as a molecular marker has widely been used for microbial analyses. However, this approach is not appropriate to investigate the denitrifying bacterial community due to the high taxonomic diversity of denitrifiers (Knowles, 1982; Zumft, 1997). Consequently, molecular research has focused on the use of functional genes involved in the denitrification pathway to investigate the abundance and diversity of denitrifiers.

As indicated in Chapter 3, during the denitrification process nitrate is reduced stepwise via four enzymatic reactions to nitrite, nitric oxide, nitrous oxide and finally to nitrogen gas. The main enzymes catalyzing each reduction step identified until now are indicated in Figure 6.1 by NAR (the membrane-bound nitrate reductase), NAP (the periplasmic nitrate reductase), Cu-NIR (the copper containing nitrite reductase), cd1-NIR (the cytrochrome cd1-containing nitrite reductase), NOR (the nitric oxide reductase) and NOS (the nitrous oxide reductase).

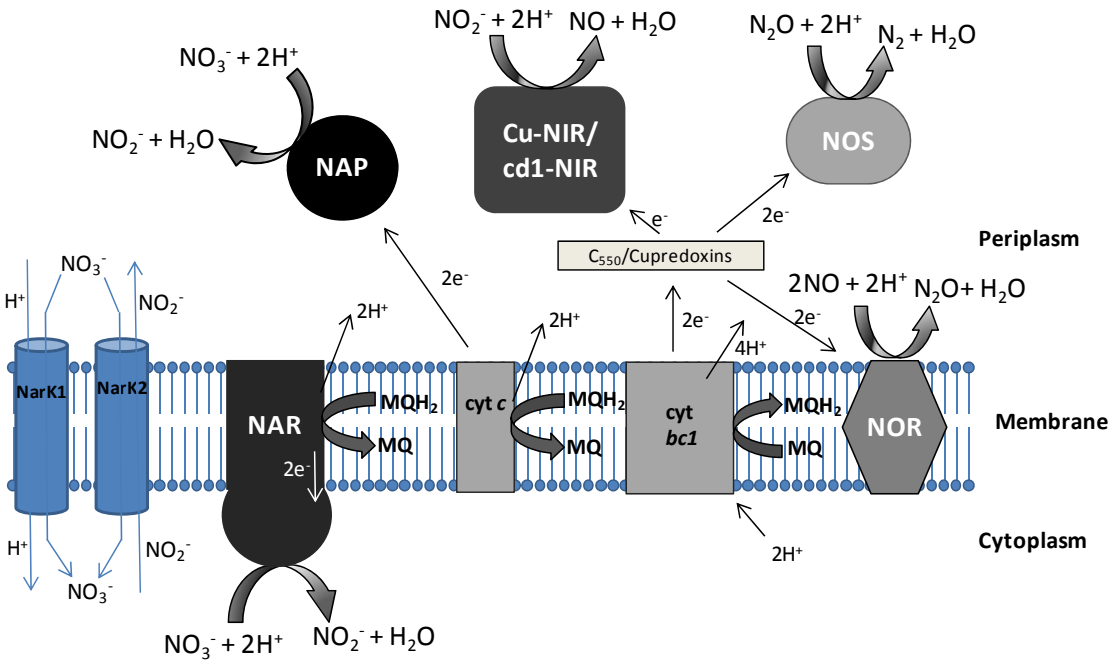

Figure 6.1. The denitrification pathway, showing the different enzymes involved in each reduction step: NAP, NAR, Cu-NIR, cd_1-NIR, NOR and NOS. cyt *bc1*: proton-pumping cytochrome bc1 complex; cyt *c*: NapC membrane-bound tetrahaem cytochrome c; cyt c_{550}: cytochrome c550; MQH2/M1: menanquinol/menanquinone pool. Adapted from Cabello *et al.* (2004).

The genes (indicated in italics) encoding the denitrifying enzymes have been described and DNA probes and primers have been developed to target them (Groffman *et al.*, 2006; Wallenstein *et al.*, 2006). It is important to underline that bacteria in the environment can

possess genes for only few steps of the denitrifying pathway or different genes for the same step.

The *nirK* and *nirS* genes, encoding Cu-NIR and cd1-NIR, respectively, have been the most common molecular markers used in denitrifier community studies (Henry *et al.*, 2004; Kandeler *et al.*, 2006; Philippot *et al.*, 2002). The reason of its extended use is due to the crucial importance of the nitrite reductase in the denitrification process, since it catalyzes the first step that leads to a gaseous product (i.e. nitric oxide).

Other authors have used the periplasmic and membrane bound nitrate reductase genes (*napA* and *narG*) encoding NAP and NAR enzymes, respectively, to investigate denitrifying bacteria in the environment (López-Gutiérrez *et al.*, 2004; Philippot *et al.*, 2002). Since these genes may be involved in denitrification as well as dissimilatory nitrate reduction to ammonia (DNRA), they have not evolved much interest in the investigation of denitrification.

Recently, denitrification has also received considerable interest because may lead to nitrous oxide emission, which is a gas involved in the global warming and the stratospheric ozone depletion (Bange, 2000; Lashof and Ahuja, 1990). It is believed that the incomplete denitrification to nitrogen gas and, therefore, nitrous oxide emission by denitrifiers may be due not only to the regulation of nitrous oxide reductase activity but also to an absence of genes encoding this enzyme in some denitrifying bacteria (Henry *et al.*, 2006). In order to investigate the production and further reduction of nitrous oxide, studies targeting the *norB* gene encoding NOR and the *nosZ* gene encoding NOS have been reported (Braker and Tiedje, 2003; Dandie *et al.*, 2007; Henry *et al.*, 2006; Saleh-Lakha *et al.*, 2008; Throback *et al.*, 2004).

In general, molecular studies in the denitrification field have been applied to investigate the abundance and diversity of denitrifiers. On the one hand, the abundance has been assessed by different molecular techniques such as direct DNA probing (e.g. Mergel *et al.*, 2001) or quantitative Polymerase Chain Reaction (qPCR, also referred as real-time PCR) (Henry *et al.*, 2004; Kandeler *et al.*, 2006), among others. On the other hand, community-level information has been mainly obtained by analyses of PCR products by fingerprinting techniques such as Terminal Restriction Fragment Length Polymorphism (T-RFLP) or Denaturing Gradient Gel Electrophoresis (DGGE) (Chèneby *et al.*, 2000; Ruiz-Rueda *et al.*, 2009).

Molecular techniques are a promising approach in the bioremediation field and, in particular, in the denitrification investigation, since they permit the accurate detection and quantification of microorganisms. Furthermore, these methods are useful to study the factors influencing

most significantly on microbial communities. In this way, recent literature points out the need to link these techniques to bioremediation tests in laboratory- or field- scales (Illman and Alvarez, 2009; Lovley, 2003). However, in denitrification literature most molecular studies are based so far on the investigation of the abundance and diversity of denitrifiers in the environment (e.g. Henry *et al.*, 2006; Kandeler *et al.*, 2006) and relatively few works are found using molecular techniques coupled to bioremediation investigation (Dandie *et al.*, 2007; Saleh-Lakha *et al.*, 2008).

2. OBJECTIVES

The main goal of this chapter is to apply molecular techniques to further study the denitrification process in the dynamic experiment detailed in Chapter 5. In order to achieve this goal, four different specific objectives are proposed:

- To develop and optimize real-time PCR assays to quantify the abundance of the total eubacterial population and denitrifying bacteria in aquifer samples.
- To study the growth and adaptability of the microbial population inside the experimental column by real-time PCR assays.
- To apply the fingerprinting technique of DGGE to study the diversity of the total eubacterial population in column samples as well as to investigate changes in the microbial community related to the amendment with an organic carbon source.
- To sequence the most prominent DGGE bands to study the taxonomic affiliation of the eubacterial population present in column samples.

3. MATERIALS AND METHODS

All the experimental procedure detailed in this chapter was carried out in the Environmental Microbiology Laboratory of GIRO Technological Centre (Organic Integrated Waste Management) in Mollet del Vallès, Catalunya (Spain).

As detailed above, real-time PCR and DGGE techniques were used to assess the quantity and diversity of the microbial population, and in particular of denitrifiers, in aquifer samples. A detailed description of both methods is provided in Chapter 1 (section 4.2) and, for a better comprehension, a schematic overview of these methods is depicted in Figure 6.2.

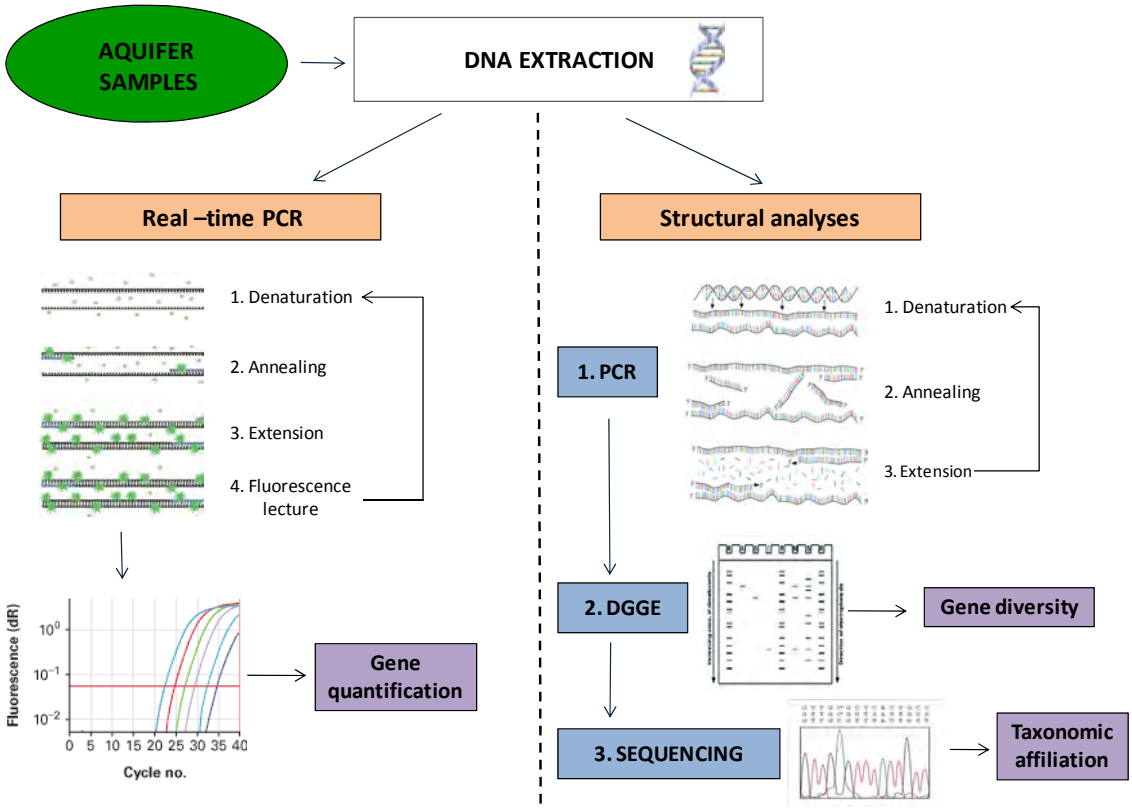

Figure 6.2. Schematic overview of the molecular techniques used in this work: real-time PCR and DGGE.

3.1. DEVELOPMENT OF REAL-TIME PCR ASSAYS

Real-time PCR assays to detect and quantify the total eubacterial population and the denitrifying population in aquifer samples were developed. On the one hand, total eubacterial population was studied by means of the 16S rRNA gene. On the other hand, two different genes involved in the denitrification pathway were selected as molecular markers to quantify the denitrifying population: the *narG* and the *nosZ* genes. The *narG* was selected because it is involved in the first step of the denitrification process, the reduction of nitrate into nitrite. However, as previously mentioned, it is known that some nitrate-reducers are involved in the DNRA process more than in the denitrification process and, therefore, the quantification of this gene usually results in an overestimation of the denitrifying population. Moreover, the selection of the *nosZ* gene was also based on its crucial importance in the denitrification process, because it encodes the enzyme responsible of the last step of the denitrification, the reduction of nitrous oxide to nitrogen gas. It is known that this enzyme lacks in some denitrifiers, but its presence ensures the potential of the denitrification to be completed. It should be mentioned that in this work, the complete reduction of nitrate to nitrogen gas was

not chemically proved and, as such, the detection and quantification of the *nosZ* gene was pointed as a main objective.

Environmental DNA usually presents inhibitors or other compounds which may interfere with PCR. In order to guarantee good results, previous optimization of real-time PCR was required to find the optimum conditions of gene amplification. In this section, the different steps followed to ensure the specificity and sensitivity of real-time PCR assays targeting 16S rRNA, *narG* and *nosZ* genes in aquifer samples are described.

3.1.1. Environmental samples

The specificity and sensitivity of the real-time PCR assays were investigated with two different types of environmental samples: groundwater and soil. Both samples had been collected on the studied site (Chapter 3, section 3.1) and were tested after running a microcosm test amended with glucose to promote denitrification (Table 6.1). Briefly, once nitrate was depleted in the feasibility heterotrophic microcosm test (Chapter 3, section 3.4.1), 100 mL groundwater were withdrawn and filtered through a 0.22 µm sterile cellulose acetate membrane filter using a filter holder (Swinnex, Millipore). Furthermore, 2 g of soil sample (wet basis) were collected. The filter and soil were brought into 10-mL sterile plastic vials and stored at -20°C until DNA extraction.

Table 6.1. Samples used in the optimization of real-time PCR assays.

Sample name	Description
GW_0	100 mL groundwater sample collected after enhanced denitrification
S_0	2 g soil sample collected after enhanced denitrification

3.1.2. DNA extraction

DNA was extracted directly from the 0.22 µm filter, obtained after filtration of 100-mL groundwater, or from 250-mg aliquot of the soil sample (wet basis), with the PowerSoil DNA isolation kit (MOBIO Laboratories, Inc.), following the manufacturer's instructions. Water content in the soil sample was measured by drying overnight at 105°C (Chapter 3, section 3.3.1) in order to express the real-time PCR results in dry basis.

Quality of DNA extracts was analysed by agarose gel electrophoresis 1% (wt/vol) in 0.5X TBE, at the constant voltage of 70V for 1h, followed by 30 min of staining with 3X GelRed (Invitrogen). The gel was visualized using a GeneFlash system (Syngene Bio Imaging). Moreover, the

quantity of DNA extracts was checked with a NanoDrop ND-1000 spectrophotometer (NanoDrop Technologies, Inc.).

3.1.3. Primers

Primers used in this study are described in Table 6.2. Quantification of the total eubacterial population was performed by means of a universal primer set proposed by Lane (1991).The primer set proposed by López-Gutiérrez *et al.* (2004), which targets a specific group of *narG* nitrate-reducers, was used to amplify a 110-bp *narG* fragment. Although this primer set is not universal, it has been used in several works (Henry *et al.*, 2006; Kandeler *et al.*, 2006) since the target nitrate-reducing group appeared to be numerically important in the environment (López-Gutiérrez *et al.*, 2004). Concerning the *nosZ*, two different primer pairs proposed by Henry *et al.* (2006), nosZ1F-nosZ1R and nosZ2F-nosZ2R were tested to amplify a 259- and a 267-bp *nosZ* fragment, respectively.

Table 6.2. Overview of PCR primers used in this study.

Primers	Targeted gene	Primer sequence (5'-3')	Reference
519f	16S rRNA	GCCAGCAGCCGCGGTAAT	(Lane, 1991)
907r	16S rRNA	CCGTCAATTCCTTTGAGTTT	(Lane, 1991)
narG1960m2f	*narG*	TAYGTSGGGCAGGARAAACTG	(López-Gutiérrez *et al.*, 2004)
narG2050m2r	*narG*	CGTAGAAGAAGCTGGTGCTGTT	(López-Gutiérrez *et al.*, 2004)
nosZ1F	*nosZ*	WCSYTGTTCMTCGACAGCCAG	(Henry *et al.*, 2006)
nosZ1R	*nosZ*	ATGTCGATCARCTGVKCRTTYTC	(Henry *et al.*, 2006)
nosZ2F	*nosZ*	CGCRACGGCAASAAGGTSMSSGT	(Henry *et al.*, 2006)
nosZ2R	*nosZ*	CAKRTGCAKSGCRTGGCAGAA	(Henry *et al.*, 2006)

3.1.4. Optimization of annealing temperature

The annealing temperature, the temperature at which the primer binds the DNA, was experimentally optimised to maximize the specificity of the *narG* and *nosZ* genes amplification in environmental samples. It should be mentioned that optimization of the annealing temperature was not required in the case of 16S rRNA since the amplification of this gene has been widely studied. For both types of DNA extracts (i.e. GW_0 and S_0) a gradient temperature from 58°C to 63°C was programmed as annealing temperature in a PCR performed with a thermocycler (Mastercycler, Eppendorf). The selection of this range of

temperatures was based on previous reported studies (Henry *et al.*, 2006; López-Gutiérrez *et al.*, 2004). Thermal cycling conditions were as follows: an initial polymerase (Ex Taq Hot Start Version; Takara Bio, Inc.) activation of 5 min at 95°C, followed by 30 cycles consisting of a 1-min denaturing step at 94°C, a 1-min annealing step at a temperature between 58°C and 63°C (depending on the specified gradient) and a 45-s elongation step at 72°C. The final elongation step was extended for 10 min at 72°C.

Amplification specificity and optimal annealing temperatures were assessed by separating PCR products by electrophoresis through a 2.5% (wt/vol) agarose gel in 0.5X TBE, at the constant voltage of 70 V for 45 min. The gel was stained with 3X GelRed during 1 h and visualized using a GeneFlash system.

3.1.5. Standards

TOPO-TA plasmids containing the 16S rRNA gene and pGEM-T plasmids carrying a single copy of the *narG* or *nosZ* genes were obtained from GIRO CT collection to perform the standard curves. However, a new *narG* plasmid stock was required by cloning the gene from environmental samples.

The primer pair and conditions described by López-Gutiérrez *et al.* (2004) (Table 6.2) were used to amplify a 110-bp *narG* fragment from the DNA extract S_0. Briefly, the obtained amplicons were purified using the Wizard SV-Gel and PCR Clean-Up System (Promega) and cloned using pGEMT Easy cloning kit (Promega) according to the manufacturer's specification. The inserted clone was amplified by PCR using the specific primer pair SP6/T7 recommended by the commercial kit and following the manufacturer's instructions. Presence, specificity and length of the inserted amplicon were assessed by agarose gel electrophoresis 1.5% (wt/vol) in 0.5X TBE, at the constant voltage of 70 V for 1 h. The gel was stained with 3X GelRed during 30 min. Finally, selection of the clone with the gene of interest was allowed and plasmid DNA was then extracted using the Wizard Miniprep Kit (Promega) according to the protocol of the manufacturer.

Gene copy numbers of the three plasmid stocks were calculated directly from the concentration, measured using NanoDrop, and the length (in base pairs) of the plasmid DNA as indicated in equation 6.1. An average molecular weight of 660 was assumed for one base pair in double stranded DNA:

$$Gene\ copies/\mu L = \frac{DNA\ concentration\ (ng/\mu L) \times 6.023 \cdot 10^{23} copies/mol}{(plasmid\ size\ (bp) \times 660 g/mol\ \times 10^{9})} \quad (6.1)$$

3.1.6. Standard curves and DNA quantification

qPCRs were carried out in a real-time thermocycler (MX3000P, Stratagene) using SYBR Green as detection system. Two different commercial master mixes were tested, the SYBR Premix Ex Taq (Perfect Real Time, Takara Bio, Inc.) and the Brilliant II SYBR Green qPCR Master Mix (Strategene). In both cases, 25-µL reaction mixtures were prepared containing 12.5 µL of the master mix, 0.5 µL of each primer, 0.5 µL ROX, 2 µL of DNA template and nuclease-free PCR-grade water to adjust the volume.

Optimization of the protocols was performed by running the standard curves. Ten-fold serial dilutions of the DNA plasmid stocks ranging from 10^1 to 10^9 were used as template, by duplicate, to determine the calibration curves. Calibration curves were obtained by plotting the threshold cycle (Ct) (i.e. the cycle number at which the fluorescence intensity reached a threshold value) versus the log of the copy numbers of the target DNA. Reaction efficiencies (E) were calculated from the slopes (M) of the calibration curves according to the following formula (Mackay, 2007):

$$E = 10^{(-1/M)} - 1 \quad (6.2)$$

Melting curve analyses of the PCR products were conducted following the real-time PCR assays to confirm that the fluorescence signal was originated from specific PCR products and not from primer-dimers or other artifacts. For the melting curves, the temperature was increased from 55 to 95°C, at a rate of 0.2°C·s^{-1}, and fluorescence data was continuously collected.

By comparing the efficiency of the calibration curves and the specificity of the assay with both types of master mixes, optimised protocols for each target gene were derived. These protocols were finally tested on the environmental samples (Table 6.1). Each sample was run in duplicate with a calibration curve and no-template-controls (NTC). In addition, presence of possible PCR inhibitors in the samples was tested by quantifying the target genes in serial dilutions of DNA extracts. The number of targeted gene copies per gram of soil or millilitre of groundwater was then calculated as follows:

$$Gene\ copies/mL\ or\ g\ soil = \frac{gene\ copies\ per\ reaction\ mix/\mu L\ template\ \times volume\ of\ DNA\ (\mu L) \times DF\ of\ DNA}{g\ or\ mL\ sample} \quad (6.3)$$

in which the number of gene copies per reaction mix was determined from the calibration curve, based on the cycle number at the set threshold fluorescence intensity (i.e. Ct), the volume of DNA retrieved from the samples was 100 µL and DF refers to the dilution factor applied to DNA template.

3.2. QUANTITATIVE DETECTION OF 16S rRNA AND *nosZ* GENES: APPLICATION TO THE COLUMN TEST

Real-time PCR analyses targeting the 16S rRNA and *nosZ* genes were performed to study the growth of the total eubacterial population and denitrifiers in the experimental soil column detailed in Chapter 5. With this purpose, 100 mL water samples before the entrance to the column (i.e. influent solution) and at the outlet of the column (26 cm height) were collected and filtered through a 0.22 µm sterile cellulose acetate membrane filter. The sampling was performed during Phase V (day 87) of column operation, in which highly nitrate-contaminated groundwater amended with glucose was pumped into the column at a flow rate of 5.4 $mL \cdot h^{-1}$ and complete denitrification was observed inside the column (Chapter 5, section 4.2). In addition, soil samples (2 g wet basis) were collected before and after column operation. Once the dynamic experiment was finished, the bottom lid of the column was opened and soil close to the water inlet was collected using a sterile spatula. All the samples were collected *in duplo* and stored in 10-mL sterile plastic vials at -20°C until molecular analyses. A detailed description of each sample is provided in Table 6.3.

Table 6.3. Column samples collected for real-time PCR assays.

Sample name	Description
col_GW1	Influent groundwater (collected during Phase V of column operation)
col_GW2	Effluent groundwater (collected during Phase V of column operation)
col_S1	Soil before packing into the column
col_S2	Soil from the bottom of the column (collected after column operation)

DNA was extracted from filters or 250-mg aliquots soil samples by using the PowerSoil DNA isolation kit. The quality and quantity of extracted DNA was assessed by agarose gel electrophoresis and by using NanoDrop, as previously described.

Two independent real-time PCR assays targeting 16S rRNA and *nosZ* genes were performed on each DNA extract (Table 6.3). The standard curves were prepared from plasmid serial dilutions

containing between 10^2 and 10^9 16S rRNA or *nosZ* copies. The assays were carried out in a real-time thermocycler MX3000P following the optimised conditions found in this work. Undiluted and 10-fold diluted DNA extracts were used as template.

For each sample replicate, qPCR was performed twice for each gene. Replicate results of qPCR measurements were averaged and the standard error was calculated.

3.3. DGGE ANALYSIS OF 16S rRNA

PCR-DGGE of 16S rRNA was used to study the microbial diversity in soil and groundwater samples from the column test. The samples assayed by DGGE are detailed in Table 6.4. As it can be observed, samples analysed by real-time PCR (Table 6.3) were also assessed by DGGE. Furthermore, two additional soil samples were collected to investigate the spatial changes of the microbial community along the height of the column: soil from the top of the column and soil at 6 cm height.

Table 6.4. Column samples collected for DGGE analyses.

Sample name	Description
col_GW1[a]	Influent groundwater (collected during Phase V of column operation)
col_GW2[a]	Effluent groundwater (collected during Phase V of column operation)
col_S1[a]	Soil before packing into the column
col_S2[a]	Soil from the bottom of the column (collected after column operation)
col_S3	Soil at 6 cm height of the column (collected after column operation)
col_S4	Soil from the top of the column (i.e. 26 cm) (collected after column operation)

[a] Correspond to the same samples assayed by real-time PCR (Table 6.3).

DNA extractions were performed as previously detailed (section 3.1.2). 16S rRNA hypervariable regions V3 to V5 were amplified by PCR using the primer set 16F341 (5'_CCT ACG GGA GGC AGC AG_3') and 16R907 (5'_CCG TCA ATT CCT TTR AGT TT_3'). PCR reactions were performed in 25 µL reactions with either 1 µL DNA template (dilution 1:100), 0.125 µL Takara Ex Taq Hot Start Version (Takara Bio, Inc.), 0.5 µL Ex Taq buffer (2mM $MgCl_2$), 200 µM of each deoxynucleoside triphosphate and 0.5 µM of forward and reverse primers. The following PCR conditions were used: an initial denaturation and enzyme activation of 5 min at 94°C, followed by 30 cycles of 1 min at 94°C, 1 min at 55°C and 45 s at 72°C, and a final extension of 10 min at 72°C. PCR was performed with a thermal cycler Mastercycler.

DGGE, based on the protocol described by Muyzer *et al.* (1993), was performed to separate the 16S rRNA amplicons. An 8% (wt/vol) polyacrylamide gel with a denaturing gradient of 30-70% (where 100% denaturant contained 7 M urea and 40% formamide) was loaded with 20 µL of the PCR products. Electrophoresis was performed at a constant voltage of 100 V for 16 h, at 60°C on a DGGE 4001 system (CBS Scientific Company, Inc.). The gels were stained with SYBR Gold (Molecular Probes Europe, Invitrogen Corporation) and digitalized with a GeneFlash system.

3.4. SEQUENCING AND PHYLOGENETIC ANALYSES

DGGE bands for sequencing were selected according to the emergence or disappearance of particular bands in the samples. Prominent bands were excised with sterile pipette tips and suspended in 50 µL of sterile deionized water overnight at 4°C. Eluted DNA fragments were re-amplified by PCR as previously detailed.

PCR products were purified for sequencing with the Wizard SV-Gel and PCR Clean-Up System according to the manufacturer's instructions. DNA sequencing reaction was carried out in a thermocycler (Mastercycler) using an ABI BigDye terminatior v3.1 cycle sequencing kit (Applied Biosystems) as specified by the manufacturer. The primers used were the R907 and the conditions of the amplification were as follows: an initial denaturation step of 1 min at 96°C, followed by 25 cycles of 10 s at 96°C, 5 s at 55°C and 4 min at 60°C. Lecture of the sequencing reaction was performed by the Scientific-Technical Services of the University of Barcelona (SCT-UB) using an ABI Prism 3700 DNA analyzer (Applied Biosystems).

Raw sequence data were checked and analysed with the BioEdit (version 7.0) software package (Hall, 1999). Sequences were compared with those deposited in the GenBank (NCBI) database by using the BLAST search alignment tool (BLASTN) software to find the closest sequence match (http://blast.ncbi.nlm.nih.gov/Blast.cgi). Furthermore, similarities between the obtained sequences were searched using the CLUSTALW software (http://www.ebi.ac.uk) in order to find possible identical sequences.

4. RESULTS AND DISCUSSION

4.1. DEVELOPMENT OF OPTIMISED PROTOCOLS FOR REAL-TIME PCR ASSAYS TARGETING 16S rRNA, *narG* AND *nosZ* GENES IN AQUIFER SAMPLES

In this section, main results of the development of real-time PCR assays to detect and quantify the total eubacterial population by means of the 16S rRNA gene and the denitrifying population, through the *narG* and the *nosZ* genes in environmental samples are reported. In addition, quantitative detection of these genes in groundwater and soil samples after running enhanced denitrification in a microcosm test is presented.

4.1.1. Environmental samples

DNA was successfully extracted from filter and soil samples by using the PowerSoil DNA isolation kit. Results from gel electrophoresis revealed that DNA extracts were not fragmented, demonstrating the feasibility to further analyse them by molecular methods. However, spectrophotometric analyses indicated the presence of other compounds (absorbance between 220-240 nm) which could affect the PCR efficiency; therefore, the optimization of qPCR assays for environmental samples was required.

4.1.2. Primer specificity and annealing temperature optimization

The specificity of the selected *narG* and *nosZ* primers (Table 6.2) in environmental and plasmid DNA was tested by PCR and gel electrophoresis analyses. In addition, different annealing temperatures of these primers were evaluated in the interval between 58 and 63°C as previously indicated.

Agarose gel electrophoresis images of the obtained PCR products in environmental samples and plasmid DNA are shown in Figure 6.3. From these images, it was observed that the DNA plasmids containing the *narG* gene (NarG_plasmid_GIRO) were not properly amplified (i.e. 110-bp PCR products were not observed), indicating that a new plasmid stock had to be obtained by cloning the gene from aquifer samples. Moreover, as previously mentioned, amplification of *nosZ* gene was tested using two different primer sets: NosZ1F/NosZ1R (NosZ1_Plasmid_GIRO) and NosZ2F/NosZ2R (NosZ2_Plasmid_GIRO). The first primer set showed more specific amplifications (259-bp PCR products) and, as such, was preferred for

further analyses. Finally, results indicated that some non-specific bands disappeared at annealing temperatures around 62 and 63°C for *narG* and *nosZ*, respectively. Therefore, these temperatures were selected to guarantee the specificity of the amplification in further analyses.

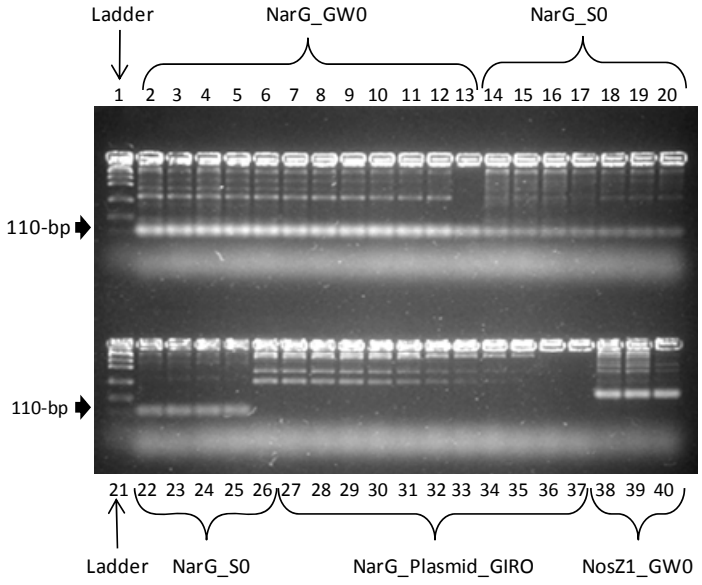

Well	annealing temperature	Well	annealing temperature
1	--	21	--
2	57.9	22	62.0
3	58.0	23	62.5
4	58.3	24	62.9
5	58.7	25	63.2
6	59.3	26	57.9
7	60.0	27	58.0
8	60.6	28	58.3
9	61.3	29	58.7
10	62.0	30	59.3
11	62.5	31	60.0
12	62.9	32	60.6
13	63.2	33	61.3
14	57.9	34	62.0
15	58.0	35	62.5
16	58.3	36	62.9
17	59.3	37	63.2
18	60.0	38	57.9
19	60.6	39	58.0
20	61.3	40	58.3

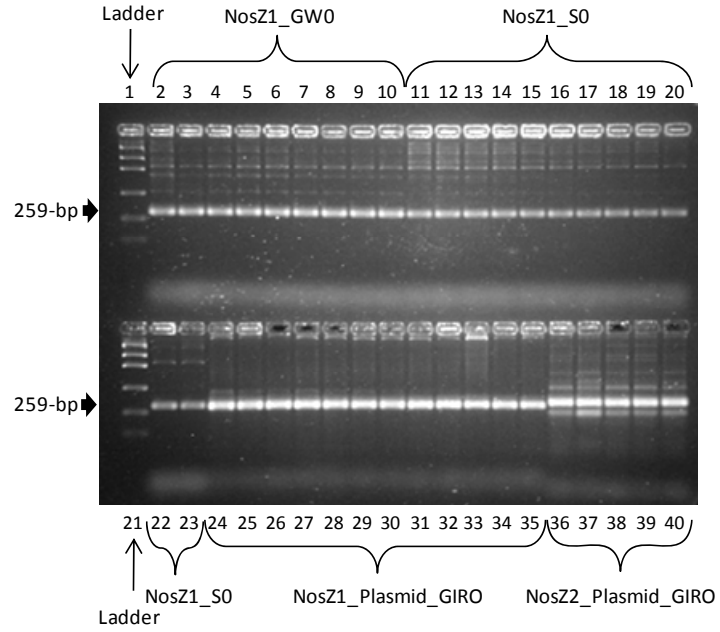

Well	annealing temperature	Well	annealing temperature
1	--	21	--
2	58.7	22	62.9
3	59.3	23	63.2
4	60.0	24	57.9
5	60.6	25	58.0
6	61.3	26	58.3
7	62.0	27	58.7
8	62.5	28	59.3
9	62.9	29	60
10	63.2	30	60.6
11	57.9	31	61.3
12	58.0	32	62
13	58.3	33	62.5
14	58.7	34	62.9
15	59.3	35	63.2
16	60.0	36	57.9
17	60.6	37	58.0
18	61.3	38	58.3
19	62.0	39	58.7
20	62.5	40	59.3

Figure 6.3. Effect of annealing temperature (58-63°C) on *narG* and *nosZ* gene amplification by PCR in environmental and plasmid DNA.

4.1.3. Optimised protocols for real-time PCR assays targeting 16S rRNA, *narG* and *nosZ*

An overview of the optimised protocols derived in this work is shown in Table 6.5, with indication of the applied concentration of each primer. As it can be observed, the master mix Brilliant II was preferred for analyses since its use resulted in a better efficiency in genes amplification than the SYBR Premix.

Table 6.5. Overview of qPCR optimised conditions used for calibration curve and further analyses.

gene → / condition ↓	16S rRNA	*narG*	*nosZ*
Primers Forward	200nM (519F)	200nM (narG1960F)	200nM (NosZ1F)
Primers Reverse	200nM (907F)	200nM (narG2050R)	200nM (NosZ1R)
Master mix	Brilliant II (Stratagene)	Brilliant II (Stratagene)	Brilliant II (Stratagene)
ROX (reference dye)	+	+	+
Enzyme activation	95°C 10 min	95°C 10 min	95°C 10 min
Denaturation	95°C 30 s	95°C 30 s	95°C 30 s
Annealing (+ Extension)	50°C 30 s	63°C 1 min	62°C 1 min
Extension	72°C 45 s		
Fluorescence lecture	80°C 15 s	80°C 15 s	80°C 15 s
Denaturation curve	55-95°C	55-95°C	55-95°C

Detailed results of the calibration curves obtained using the optimised conditions are shown in Table 6.6. In the three qPCR assays, there was a linear relationship between the plasmid DNA copy number and the Ct value across the tested concentration range (R^2>0.98). Amplification efficiencies, calculated by means of equation 6.2, varied from 101.7 to 104.9%. Calibrating curves were performed in duplicate and relative standard errors (RSD) were observed to be between 0.01% and 3.37%.

Table 6.6. Standard curves and reaction efficiencies.

Gen	Slope	Intercept	Efficiency	R^2	RSD (%)
16S rRNA	-3.227	35.96	104.1	0.996	0.02-3.37
narG	-3.210	36.24	104.9	0.994	0.01-1.12
nosZ	-3.283	41.23	101.7	0.989	0.39-1.98

Melting curve analyses with target genes from plasmid DNA showed one distinct peak (Figure 6.4) indicating the specificity of the amplification.

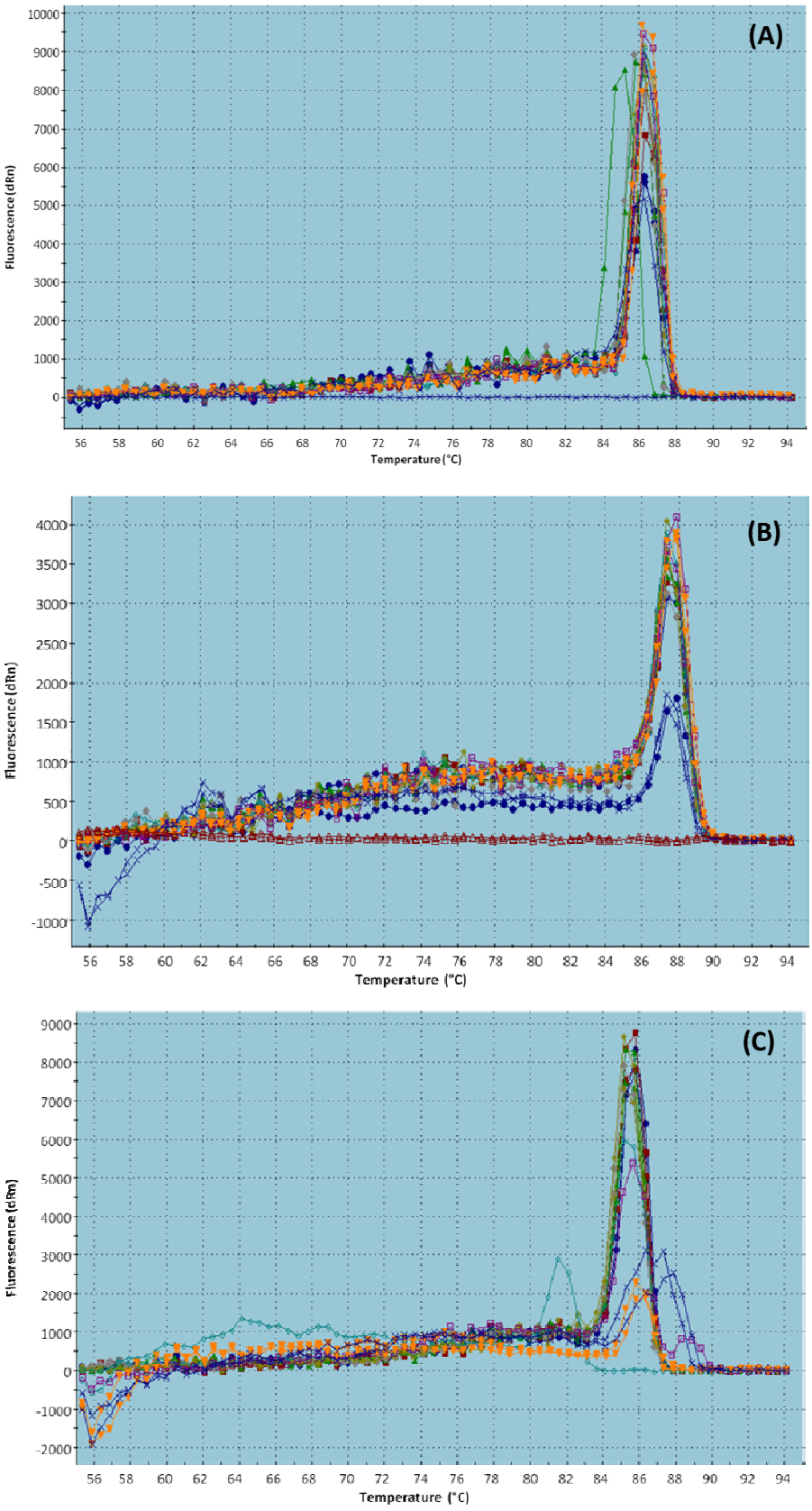

Figure 6.4. Melting curves profiles of (A) 16S rRNA, (B) *narG* and (C) *nosZ* genes performed during the calibration procedure.

4.1.4. Quantification of 16s rRNA, *narG* and *nosZ* in environmental samples

Finally, the applicability of the assays to quantify the 16S rRNA, the *narG* and the *nosZ* genes in aquifer samples was evaluated using DNA extracted from GW_0 and S_0 samples (Table 6.1). The three genes were quantified by real-time PCR on duplicate for each sample and average results are indicated in Table 6.7. All the genes in both types of samples could be adequately quantified since copy numbers were high (10^3 to 10^8) and significantly removed from the NTC signal.

It was observed that when using non-diluted DNA templates the heterogeneity of results was significantly high (RSD>50%). Therefore, results shown in Table 6.7 are from DNA templates run 10-fold diluted.

Table 6.7. Gene copies in aquifer or groundwater samples obtained by qPCR and RSD.

Sample	gene copies · g^{-1} soil (dry basis) or gene copies · mL^{-1} water [a,b]					
	16S rRNA	***RSD (%)***	***narG***	***RSD (%)***	***nosZ***	***RSD (%)***
GW_0	$(3.6 \pm 0.1)\cdot 10^6$	3.0	$(2.64 \pm 0.08)\cdot 10^4$	3.0	$(3.1 \pm 0.5)\cdot 10^3$	16.8
S_0	$(3.2 \pm 0.4)\cdot 10^8$	13.4	$(7.4 \pm 0.8)\cdot 10^5$	11.1	$(3.1 \pm 0.5)\cdot 10^5$	17.8

[a] Results are the average of reaction duplicates.
[b] NTC signal was adequately removed from sample signals before quantification.

The abundance of the *narG* nitrate-reducing bacteria was expected to be higher than the *nosZ* denitrifying population in environmental samples since it is known that *narG* is present in denitrifiers and also bacteria capable to reduce nitrate to ammonia (DNRA process), whereas some denitrifiers lack the *nosZ* gene. However, results indicated similar densities of both genes in the analysed samples. These results could be explained taking into account that the primers used to amplify the *narG* gene were not universal and results did not probably quantify the whole nitrate-reducing microbial population. This finding is in contrast with other authors who indicated that this target group of *narG* nitrate-reducers was numerically important in the environment (Chèneby *et al.*, 2003, López-Gutiérrez *et al.,* 2004). For instance, López-Gutiérrez *et al.* (2004), found in different environmental samples such as various agricultural and garden soils and river sediments, *narG* copy numbers between 10^8 and 10^{11} per gram of dry weight of environmental samples.

4.2. QUANTIFICATION OF TOTAL EUBACTERIAL AND DENITRIFYING POPULATIONS IN THE DYNAMIC DENITRIFICATION TEST BY REAL-TIME PCR

The optimised real-time PCR protocols detailed in the above section were used to quantify the abundance of 16S rRNA and *nosZ* genes in aquifer samples from the column test. In this case, *narG* was not studied since previous results indicated similar abundances of *narG* nitrate-reducers and *nosZ* denitrifiers in groundwater and soil samples. Results of 16S rRNA and *nosZ* copies obtained in soil and groundwater samples from the experimental column are detailed in Table 6.8 and Figure 6.5.

Table 6.8. Gene copies in groundwater or soil samples obtained by real-time PCR and relative abundance of the *nosZ* gene.

Sample	gene copies · g^{-1} soil (dry basis) or gene copies · mL^{-1} water [a,b]		Ratio (%) *NosZ*/16S rRNA
	16S rRNA	*nosZ*	
col_GW1	$(3.5 \pm 2.3)\cdot 10^4$	$(2.1 \pm 3.0)\cdot 10^2$	0.6
col_GW2	$(8.6 \pm 1.4)\cdot 10^5$	$(8.8 \pm 2.5)\cdot 10^4$	10.2
col_S1	$(8.8 \pm 1.2)\cdot 10^7$	$(9.4 \pm 7.7)\cdot 10^5$	1.1
col_S2	$(1.9 \pm 2.0)\cdot 10^9$	$(3.9 \pm 4.3)\cdot 10^8$	20.9

[a] Results are the average of replicates.
[b] NTC signal was adequately removed from sample signals before quantification

From the obtained results it can be observed that inside the column the growth of denitrifiers containing the *nosZ* gene was significantly higher than the growth of the total eubacterial population. The density of 16S rRNA increased 21 times from the influent (col_GW1) to the effluent (col_GW2) groundwater samples and 24 times from initial soil samples (col_S1) to soil samples at the end of column operation (col_S2). However, the density of the *nosZ* gene increased 415 from col_GW1 to col_GW2 and 417 times from col_S1 to col_S2. Expressing the copy numbers of *nosZ* gene as a percentage of 16S rRNA copy numbers, it can be observed that in the groundwater samples, denitrifiers containing the *nosZ* gene represented less than 1% of the total eubacterial population in the influent groundwater, whereas in the effluent groundwater they represented more than 10%. With regard to the soil samples, the same trend was observed. In the initial soil sample, the relative abundance of *nosZ* gene was only about 1%, while in the column soil sample was more than 20% of 16S rRNA gene copies. Interestingly, the obtained result of relative abundance of the *nosZ* gene in the initial soil

sample (col_S1) was roughly in the same order as previously reported in other agricultural soils (0.2-3%) (Henry *et al.*, 2006).

It should be mentioned that, again, it was observed that the use of non-diluted DNA template resulted in a high heterogeneity in qPCR results. Therefore, results detailed in Table 6.8 were obtained from DNA templates ten-fold diluted. Nevertheless, heterogeneity between sample duplicates was also important, RSD in the 16S rRNA and *nosZ* quantification were between 13-105% and 29-142%, respectively. However, reaction duplicates showed lower RSD, between 0.10 and 5.60% for 16S rRNA gene and between 0.03 and 2.37% for the n*osZ* gene. Therefore, main dispersion was due to heterogeneity between samples duplicates more than reaction duplicates. This heterogeneity could be explained due to the intrinsic granulometry of soil samples. Furthermore, in groundwater samples, specially from column outlet, the different presence of soil particles may have caused the observed dispersion.

According to the NTC, the detection limits were calculated to be $1.1 \cdot 10^2$ (16S rRNA) and $4.3 \cdot 10^1$ (*nosZ)* copies per milliliter groundwater and $4.4 \cdot 10^4$ (16S rRNA) and $1.7 \cdot 10^4$ (*nosZ*) copies per gram dry weight soil.

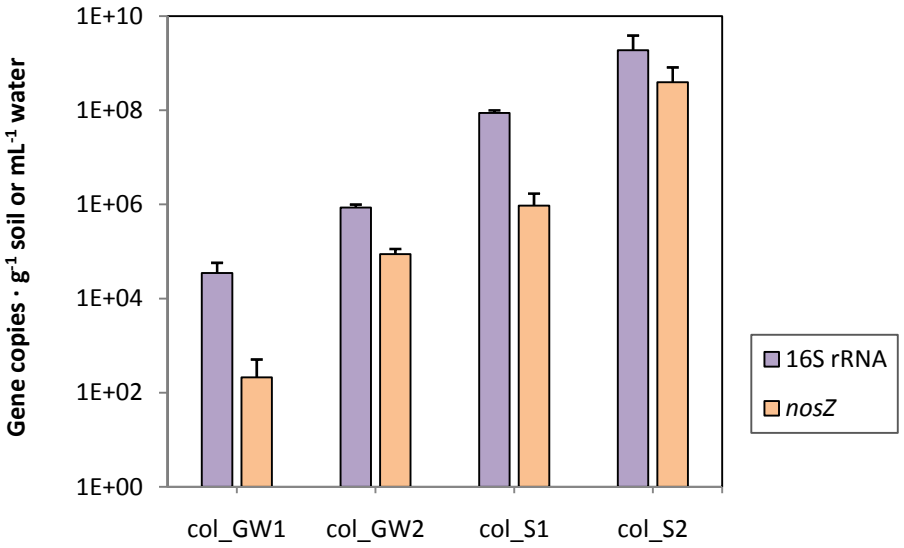

Figure 6.5. 16S rRNA and *nosZ* copies · g^{-1} of dry soil or mL^{-1} of groundwater in the different assayed samples (Table 6.3). Error bars are the standard errors of the mean for the replicates.

Until now, for denitrifying genes, only single copies per genome have been reported, with the exception of the *narG* gene, which can be present in up to three copies (Kandeler *et al.*, 2006; Philippot, 2002). Therefore, from the obtained results, it can be assumed that densities of *nosZ* denitrifiers in soil collected on 2009 were in the range of 10^5 bacteria per gram of dry weight

soil. This result is slightly higher than the initial denitrifying population estimated by Most Probable Number (MPN in the range of 10^4 bacteria per gram of dry weight soil). Although the analyses by MPN and qPCR were not performed at the same time and, therefore, could not be properly compared, this finding could indicate that the MPN method underestimates the number of denitrifiers, as previous reported by other authors (Henry *et al.*, 2004; Michotey *et al.*, 2000).

Overall, it can be concluded that the stimulation of the soil material with glucose in the column test resulted in an increase of the microbial population and, in particular, of the denitrifying bacteria. It is also important to note that the increase of *nosZ*- denitrifiers is an indication that nitrate may be completely reduced to nitrogen gas. Nevertheless, it is important to stress that the presence of the gene sequence indicates the potential presence of the corresponding function, but there is evidence that this potential is not always converted to an actual metabolic rate (Philippot *et al.*, 2002).

4.3. MICROBIAL COMMUNITY STUDY IN THE DYNAMIC DENITRIFICATION TEST BY DGEE

The DGGE band pattern of 16S rRNA from aquifer samples after column operation was completely different from initial aquifer samples (Figure 6.6). Thus, it can be concluded that glucose amendment affected the indigenous eubacterial population.

Differences between influent (col_GW1) and effluent (col_GW2) groundwater samples were observed (Figure 6.6), indicating that in nitrate-treated water a different eubacterial pattern was present. With regard to soil samples, it is important to note that initial soil samples (col_S1) presented a diffuse DGGE band pattern, typically observed in natural soils. A similar pattern was obtained in soil samples from the top of the column (col_S4) corroborating, as observed in Chapter 5, that the growth of microorganisms took place in the first soil layers of the column where complete nitrate, oxygen and glucose removal was attained. In fact, main emerging bands were observed in the soil samples from first centimetres of the column (col_S2 and col_S3).

Sixteen bands were gel excised (Figure 6.6), and ten of them could be finally sequenced. Best matches with the GenBank database are detailed in Table 6.9. It is important to note that sequences obtained were mainly belonging to Betaproteobacteria class, and in particular to the Comamonadaceae family within the order of Burkholderiales. In addition, sequences

belonging to Bacteroidetes phylum, in particular to the family of Flavobacteriaceae, were also detected. Interestingly, all the identified species, except *Polaromonas* sp., have been described as potential denitrifiers (Holt *et al.*, 1994).

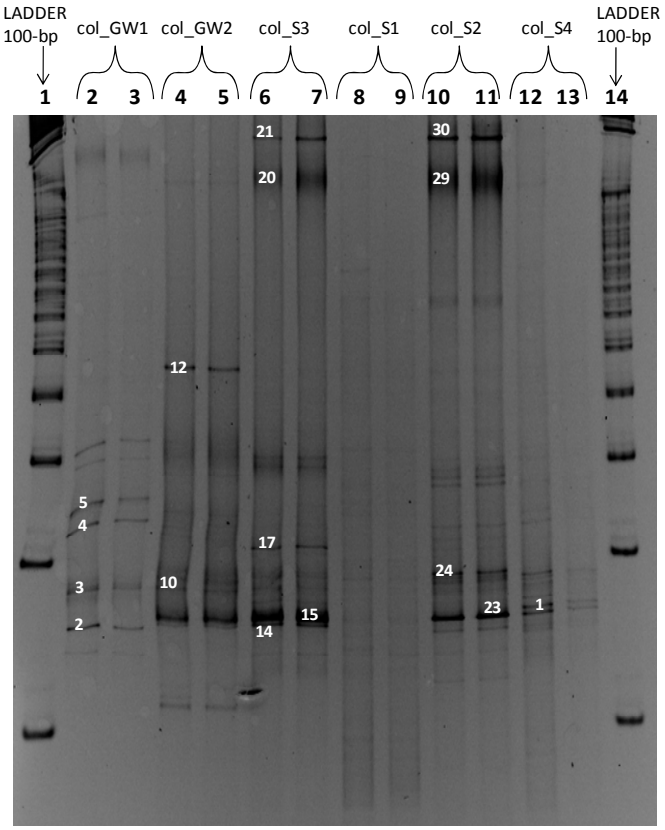

Figure 6.6. DGGE profiles of PCR-amplified 16S rRNA gene fragments from groundwater and soil samples of the column test. Numbers indicate the identity of excised bands.

Results from the alignment study performed by CLUSTALW revealed that bands 20/21 and 29/30 corresponded to the same sequence, whereas bands 3, 15, 23 were not the same sequence, although they presented a high similarity.

Overall, results from DGGE analyses demonstrated that the continuous amendment of the soil column with glucose influenced the indigenous bacterial diversity present in aquifer samples. Furthermore, by sequencing the prominent bands it was corroborated the enrichment with denitrifying species within the eubacterial population present in aquifer samples from the column.

Table 6.9. Bacterial 16S rRNA gene sequences obtained from soil and groundwater column samples.

DGGE band [a]	length (nt)	Best match database (GenBank accession number)	Similarity (%)	Taxonomic affiliation
B1	NA [b]	NA	NA	NA
B3	360	*Polaromonas sp.* (GU213397)	99.4	Proteobacteria/β-proteobacteria/Burkholdariales/ Comamonadaceae
B10	NA	NA	NA	NA
B12	274	Uncultured Bacteroidetes	99.3	Bacteroidetes/Sphingobacteria/Sphingobacteriales
B15	534	*Acidovorax sp.* (AM084039)	100	Proteobacteria/ β-proteobacteria/ Burkholdariales/ Comamonadaceae
B20	522	*Flavobacterium sp.* (AM934649)	100	Bacteroidetes/Flavobacteria/ Flavobacteriales/ Flavobacteriaceae
B21	422	*Flavobacterium sp.* (AM934649)	100	Bacteroidetes/Flavobacteria/ Flavobacteriales/ Flavobacteriaceae
B23	523	Uncultured bacteria (FJ175105) *Hydrogenophaga taeniospiralis* (AF078768)	100 99.8	-- Protoebacteria/β-proteobacteria/ Burkholdariales/ Comamonadaceae
B29	517	*Flavobacterium sp.* (AM934649)	100	Bacteroidetes/Flavobacteria/ Flavobacteriales/ Flavobacteriaceae
B30	422	*Flavobacterium sp.* (AM934649)	100	Bacteroidetes/Flavobacteria/ Flavobacteriales/ Flavobacteriaceae

[a] Excised bands from DGGE gel (related to Figure 6.6).
[b] NA: not available. These bands could not properly be sequenced due to an excess of indeterminations in the electrophotograms.

5. CONCLUSIONS

Real-time PCR assays to quantify the total eubacterial population by means of the 16S rRNA gene as well as the denitrifiers through the *narG* and the *nosZ* genes in aquifer samples were developed and optimised. The reproducibility and the specificity of the amplification obtained in the standard curves were good, with RSD from 0.01 to 3.37%.

The optimised real-time PCR protocols were tested to quantify the selected genes in environmental samples from the Argentona aquifer after running an enhanced denitrification test. Results of the *narG* gene seemed not to quantify the total nitrate-reducing population from the samples.

Following the optimised protocols, 16S rRNA and *nosZ* genes were quantified in groundwater and soil samples from a dynamic denitrification experiment (Chapter 5). Results demonstrated the presence of denitrifying bacteria in the effluent groundwater and the growth of the microbial population in soil samples from the bottom of the column (close to the groundwater inlet). Comparing influent and effluent groundwater samples, the relative abundance of the *nosZ* gene increased from initial 0.6 to 10.2% of 16S rRNA gene. Furthermore, the relative abundance of the *nosZ* gene was observed to increase from initial 1.1 to 20.9% of 16S rRNA genes in soil samples after column operation.

DGGE band pattern was found to reflect the change on the indigenous eubacterial population between the influent and effluent groundwater as well as in soil samples along the height of the experimental column. In particular, the band pattern in soil samples from the bottom of the column (close to the water inlet) was significantly different from initial soil samples, corroborating that main microbial activity was in first layers of the soil column

Sequencing of prominent 16S rRNA DGGE bands corroborated the increase of denitrifiers among the eubacterial population present in the soil column amended with glucose.

In general, qPCR and DGGE results demonstrated the importance of not only following the chemical contaminants when applying bioremediation but also of studying the microbial populations to better assess the feasibility of the bioremediation treatment.

6. REFERENCES

Bange, H.W. 2000. Global change - It's not a gas. *Nature*, 408, 301-302.

Braker, G. and Tiedje, J.M. 2003. Nitric oxide reductase (*norB*) genes from pure cultures and environmental samples. *Applied and Environmental Microbiology*, 69, 3476-3483.

Cabello, P., Roldan, M.D. and Moreno-Vivian, C. 2004. Nitrate reduction and the nitrogen cycle in archaea. *Microbiology-Sgm*, 150, 3527-3546.

Chèneby, D., Philippot, L., Hartmann, A., Henault, C. and Germon, J.C. 2000. 16S rDNA analysis for characterization of denitrifying bacteria isolated from three agricultural soils. *FEMS Microbiology Ecology*, 34, 121-128.

Chèneby, D., Hallet, S., Mondon, M., Martin-Laurent, F., Germon, J.C. and Philippot, L. 2003. Genetic characterization of the nitrate reducing community based on *narG* nucleotide sequence analysis. *Microbial Ecology*, 46, 113-121.

Dandie, C.E., Miller, M.N., Burton, D.L., Zebarth, B.J., Trevors, J.T. and Goyer, C. 2007. Nitric oxide reductase-targeted real-time PCR quantification of denitrifier populations in soil. *Applied and Environmental Microbiology*, 73, 4250-4258.

Groffman, P.M., Altabet, M.A., Bohlke, J.K., Butterbach-Bahl, K., David, M.B., Firestone, M.K., Giblin, A.E., Kana, T.M., Nielsen, L.P. and Voytek, M.A. 2006. Methods for measuring denitrification: Diverse approaches to a difficult problem. *Ecological Applications*, 16, 2091-2122.

Hall, T. 1999. Biological Sequence Alignment Editor for Win95/98/NT/2K/XP. Ibis Biosicences, Carlsbad, CA.

Henry, S., Baudoin, E., Lopez-Gutierrez, J.C., Martin-Laurent, F., Baumann, A. and Philippot, L. 2004. Quantification of denitrifying bacteria in soils by *nirK* gene targeted real-time PCR. *Journal of Microbiological Methods*, 59, 327-335.

Henry, S., Bru, D., Stres, B., Hallet, S. and Philippot, L. 2006. Quantitative detection of the *nosZ* gene, encoding nitrous oxide reductase, and comparison of the abundances of 16S rRNA, narG, nirK, and nosZ genes in soils. *Applied and Environmental Microbiology*, 72, 5181-5189.

Holt, J.G., Krieg, N.R., Sneath, P.H.A., Staley, J.T., Williams, S.T. (1994). Bergey's manual of determinative bacteriology (ninth edition). Williams & Wilkins. Philadelphia, USA.

Illman, W.A. and Alvarez, P.J. 2009. Performance Assessment of Bioremediation and Natural Attenuation. *Critical Reviews in Environmental Science and Technology*, 39, 209-270.

Kandeler, E., Deiglmayr, K., Tscherko, D., Bru, D. and Philippot, L. 2006. Abundance of narG, nirS, nirK, and nosZ genes of denitrifying bacteria during primary successions of a glacier foreland. *Applied and Environmental Microbiology*, 72, 5957-5962.

Knowles, R. 1982. Denitrification. *Microbiological Reviews*, 46, 43-70.

Lane, D.J. 1991. 16S/23S rRNA sequencing, In: Stackebrandt, E., Goodfellow, M. (ed.). Nucleic acid techniques in bacterial systemics. pp.205-248.

Lashof, D.A. and Ahuja, D.R. 1990. Relative contributions of greenhouse gas emissions to global warming. *Nature*, 344, 529-531.

López-Gutiérrez, J.C., Henry, S., Hallet, S., Martin-Laurent, F., Catroux, G. and Philippot, L. 2004. Quantification of a novel group of nitrate-reducing bacteria in the environment by real-time PCR. *Journal of Microbiological Methods*, 57, 399-407.

Lovley, D.R. 2003. Cleaning up with genomics: Applying molecular biology to bioremediation. *Nature Reviews Microbiology*, 1, 35-44.

Mackay, I.M. 2007. Real-time PCR in microbiology: from diagnosis to characterisation. Caister Academic Press. Norfolk, UK.

Mergel, A., Schmitz, O., Mallmann, T. and Bothe, H. 2001. Relative abundance of denitrifying and dinitrogen-fixing bacteria in layers of a forest soil. *FEMS Microbiology Ecology*, 36, 33-42.

Michotey, V., Mejean, V. and Bonin, P. 2000. Comparison of methods for quantification of cytochrome cd(1)-denitrifying bacteria in environmental marine samples. *Applied and Environmental Microbiology*, 66, 1564-1571.

Muyzer, G., Dewaal, E.C. and Uitterlinden, A.G. 1993. Profiling of complex microbial-populations by denaturing gradient gel-electrophoresis analysis of polymerase chain reaction-amplified genes-coding for 16S ribosomal-RNA. *Applied and Environmental Microbiology*, 59, 695-700.

Philippot, L. 2002. Denitrifying genes in bacterial and Archaeal genomes. *Biochimica Et Biophysica Acta-Gene Structure and Expression*, 1577, 355-376.

Philippot, L., Piutti, S., Martin-Laurent, F., Hallet, S. and Germon, J.C. 2002. Molecular analysis of the nitrate-reducing community from unplanted and maize-planted soils. *Applied and Environmental Microbiology*, 68, 6121-6128.

Ruiz-Rueda, O., Hallin, S. and Baneras, L. 2009. Structure and function of denitrifying and nitrifying bacterial communities in relation to the plant species in a constructed wetland. *FEMS Microbiology Ecology*, 67, 308-319.

Saleh-Lakha, S., Shannon, K.E., Goyer, C., Trevors, J.T., Zebarth, B.J. and Burton, D.L. 2008. Nitric Oxide Reductase Gene Expression and Nitrous Oxide Production in Nitrate-Grown *Pseudomonas mandelii*. *Applied and Environmental Microbiology*, 74, 6876-6879.

Throback, I.N., Enwall, K., Jarvis, A. and Hallin, S. 2004. Reassessing PCR primers targeting nirS, nirK and nosZ genes for community surveys of denitrifying bacteria with DGGE. *Fems Microbiology Ecology*, 49, 401-417.

Wallenstein, M.D., Myrold, D.D., Firestone, M. and Voytek, M. 2006. Environmental controls on denitrifying communities and denitrification rates: Insights from molecular methods. *Ecological Applications*, 16, 2143-2152.

Zumft, W.G. 1997. Cell biology and molecular basis of denitrification. *Microbiology and Molecular Biology Reviews*, 61, 533-616.

PART II - Chapter 7

STUDY OF THE FACTORS DETERMINING THE BIODEGRADATION OF CAHs IN RIVER SEDIMENT AND AQUIFER MATERIAL

1. INTRODUCTION

Chlorinated aliphatic hydrocarbons (CAHs) such as tetrachloroethene (PCE), trichloroethene (TCE) and 1,1,1-trichloroethane (1,1,1-TCA) rank amongst the most common groundwater pollutants in industrial countries due to their widespread use as solvents and degreasing agents (Fischer *et al.*, 1987; Grostern and Edwards, 2006; Squillace *et al.*, 1999). At many industrial sites, CAH-polluted groundwater can discharge into nearby surface waters, representing a continuous source of diffuse contamination and imposing serious environmental threats (Conant *et al.*, 2004; Ellis and Rivett, 2007; Lendvay *et al.*, 1998). However, before reaching the surface waters, CAHs have to cross the interface of groundwater and surface water, commonly known as the hyporheic zone.

The term hyporheic is derived from Greek roots: *hypo*, meaning under or beneath, and *rheos* meaning a stream. To date, there is still no single conceptual definition of hyporheic zone and a number of definitions can be found in literature in function of the discipline they have arisen from. Nevertheless, some common themes in all the definitions found in literature can be summarized as: (1) it is the zone below and adjacent to a streambed in which water from the open channel exchanges with interstitial water in the bed sediments, (2) it is the zone around a stream in which characteristic fauna of the hyporheic zone is distributed and live, and (3) it is the zone in which groundwater and surface water mix (Smith, 2005).

Hyporheic zones are characterized by sharp chemical (e.g. redox) and physical gradients, dynamic exchange of oxygen, high organic carbon and nutrients availability, and a dense microbial and invertebrate community (Brunke and Gonser, 1997; Feris *et al.*, 2003; Pusch *et al.*, 1998). Such conditions may therefore be assumed to provide particularly favourable conditions for both biotic and abiotic processes effecting contaminants present in discharging groundwater.

Literature contains few studies focused on CAHs natural attenuation within the groundwater-surface water interface (Conant *et al.*, 2004; Chapman *et al.*, 2007; Ellis and Rivett, 2007; LaSage *et al.*, 2008; Lendvay *et al.*, 1998). Some of these studies have reported that abiotic processes can contribute to natural attenuation of CAHs in the hyporheic zone. For example, the high organic carbon content in streambed deposits was linked to a high degree of sorption of CAHs (Conant *et al.*, 2004). Moreover, dilution of CAHs concentration in the riverbed by infiltrating surface water or by discharging unpolluted groundwater was also suggested to contribute to CAHs attenuation in hyporheic zones (Hamonts *et al.*, 2009). Obviously, after the

discharge of the CAH plume into the surface water, quick dilution by clean river water occurred, resulting in CAH concentrations below or close to the detection limits in most river water samples (Conant *et al.*, 2004; Chapman *et al.*, 2007; Ellis and Rivett, 2007). However, higher concentrations of CAHs were detected in surface water near springs (Conant *et al.*, 2004; LaSage *et al.*, 2008). The low CAHs concentrations measured in surface waters were also partially attributed to volatilization of CAHs into the atmosphere in some studies (Chapman *et al.*, 2007; LaSage *et al.*, 2008).

In a different approach some studies have demonstrated the occurrence of biotic CAHs attenuation processes in hyporheic sediments impacted by contaminated plumes, including both anaerobic and aerobic processes. Under anaerobic conditions, halorespiring microorganisms were found to reductive dechlorinate higher chlorinated compounds such as PCE and TCE to not only lesser chlorinated compounds but also to the non toxic end products ethene and ethane (Conant *et al.*, 2004; Kuhn *et al.*, 2009; Lendvay *et al.*, 1998). As previously detailed in Chapter 1, during halorespiration, dissolved-phase chlorinated ethenes serve as electron acceptors for the dechlorinating microorganisms, while the source of electrons is typically hydrogen (Smatlak *et al.*, 1996; Yang and McCarty, 1998), supplied from the oxidation of organic substrates by fermenting microbial communities. In contrast, under aerobic conditions oxidation of CAHs, specially, less chlorinated compounds, was reported. Mineralization of dichloroethene (DCE) and vinyl chloride (VC) by microorganisms indigenous from aquifer or sediments receiving CAH-contaminated groundwater was reported by Bradley and Chapelle (1998) under both aerobic and anaerobic conditions. Furthermore, some authors have also described CAHs co-metabolic degradation. Lendvay *et al.* (1998) found evidence suggesting that reductive dechlorination of TCE to lesser chlorinated compounds, particularly VC, was the predominant transformation process in the deep methanogenic zones of a lake sediment, whereas VC was co-metabolically oxidized by methane-oxidizing microorganisms in the shallow zone of the lake sediments impacted by the infiltration of oxygenated surface waters.

2. OBJECTIVES

The aim of this chapter is to investigate the factors determining the biodegradation of CAHs in Zenne River sediments and CAH-polluted aquifer material collected near the river. Therefore, the specific purposes of this chapter are:

- To compare the intrinsic VC, *cis*-1,2-dichloroethene (*cis*-DCE) and 1,1-dichloroethane (1,1-DCA) reductive dechlorination potential of the river sediments and aquifer material by microcosm batch tests and continuous-flow column tests.
- To study the effects on CAH biodegradation of the groundwater flow rate, the presence of co-contaminants and the surface water infiltration in dynamic experiments.
- To investigate the stimulation of microorganisms from river sediments and aquifer material with different electron sources in batch and column tests.

3. MATERIALS AND METHODS

3.1. SITE DESCRIPTION

The studied field site is located in an industrial area in Vilvoorde (north of Brussels, Belgium). At this site, several spills of PCE, TCE and 1,1,1-TCA have resulted in a 1.4 km-wide groundwater plume of lower-chlorinated transformation products i.e. *cis*-DCE, VC, 1,1-DCA and chloroethane (CA). This CAH plume flows to the nearby River Zenne reaching the right riverbank, while unpolluted groundwater approaches to the opposite riverbank.

The River Zenne is 103 km long and has a basin of 1164 km^2. At the study site, the Zenne is relatively straight, 12-15 m wide, 0.5-2 m deep and has a stream flow of 5-10 $m^3 \cdot s^{-1}$ in dry weather conditions. In addition, the Zenne is dammed in this area at both sides by steel walls, resulting in a vertical discharge of the groundwater into the riverbed. The top 1.2 m of the riverbed is referred as sediment, even when its composition is analogous to the adjacent aquifer. Bed materials range from fine to coarse grained sand and gravel to silt and slick.

River Zenne receives domestic sewage at various locations, which creates highly eutrophic conditions in the surface water and the riverbed. However, it is important to mention that, from March 2007 onwards, due to sanitation of the surface water upstream of the test area, the eutrophic character of the surface water has decreased.

The surrounding aquifer is essentially all the same type of aquifer, although it is referred to as polluted aquifer at the right riverbank and as unpolluted aquifer at the left riverbank. The top 4 to 5 m of the soil consists of loamy or clayish material with low permeability, while the soil material from 5 to about 12 m below the ground surface (mbs), which forms a semi-confined aquifer, contains more permeable material such as sand and gravel (Hamonts, 2009). The groundwater flows in north-northwestern direction (N20°W). Hydraulic conductivity is about 1 to 3 $m \cdot day^{-1}$, the regional hydraulic gradient ~0.0015 $m \cdot m^{-1}$ and the calculated groundwater velocity is in the order of 2 to 60 $m \cdot year^{-1}$ (Bronders *et al.*, 2007).

Except during extreme precipitation events, when the water level of the River Zenne can exceed the groundwater level, the Zenne drains groundwater from both sides of the river. While groundwater in the CAH-polluted aquifer is primarily recharged by precipitation, groundwater recharge in the unpolluted aquifer is supplemented by seepage from the nearby canal "Brussels-Scheldt" (Figure 7.1) (Hamonts *et al.*, 2009).

3.2. SAMPLE COLLECTION

Groundwater was collected from four different monitoring wells SB-2, SB-1, PB-26 and SB-3, which are located in the test area at approximately 3.5, 28.2, 200 and 500 m distance from the right riverbank of the River Zenne (Figure 7.1). Groundwater samples were collected using a peristaltic pump and polyethylene sample tubes (Eijkelkamp). Before collecting samples, the depth of the groundwater was measured and the boreholes were properly purged until electrical conductivity, temperature, pH, dissolved oxygen (DO) and oxidation-reduction potential (ORP) parameters were stabilized. These parameters were measured using a flow-through cell (Eijkelkamp) and a multimeter (MultiLine F/SET3, WTW) equipped with electrodes for electrical conductivity and temperature (TetraCon 325, WTW), pH (Sen Tix 41, WTW), DO (CellOx 325, WTW) and ORP (Oxitrode Platinum, Hamilton). All groundwater samples were collected in 2 L glass bottles by filling them from bottom to top and allowing overflow until the volume of the bottle was changed two times.

Surface water samples from River Zenne were collected at post 26 (Figure 7.1) in 2 L glass bottles, without leaving headspace. Electrical conductivity, temperature, pH, DO and ORP were measured electrometrically *in situ*, using the multimeter and electrodes described above. River sediments were also collected at post 26 using a 4 cm diameter piston sediment sampler. Undisturbed sediment samples were transferred into PVC bottles on the field.

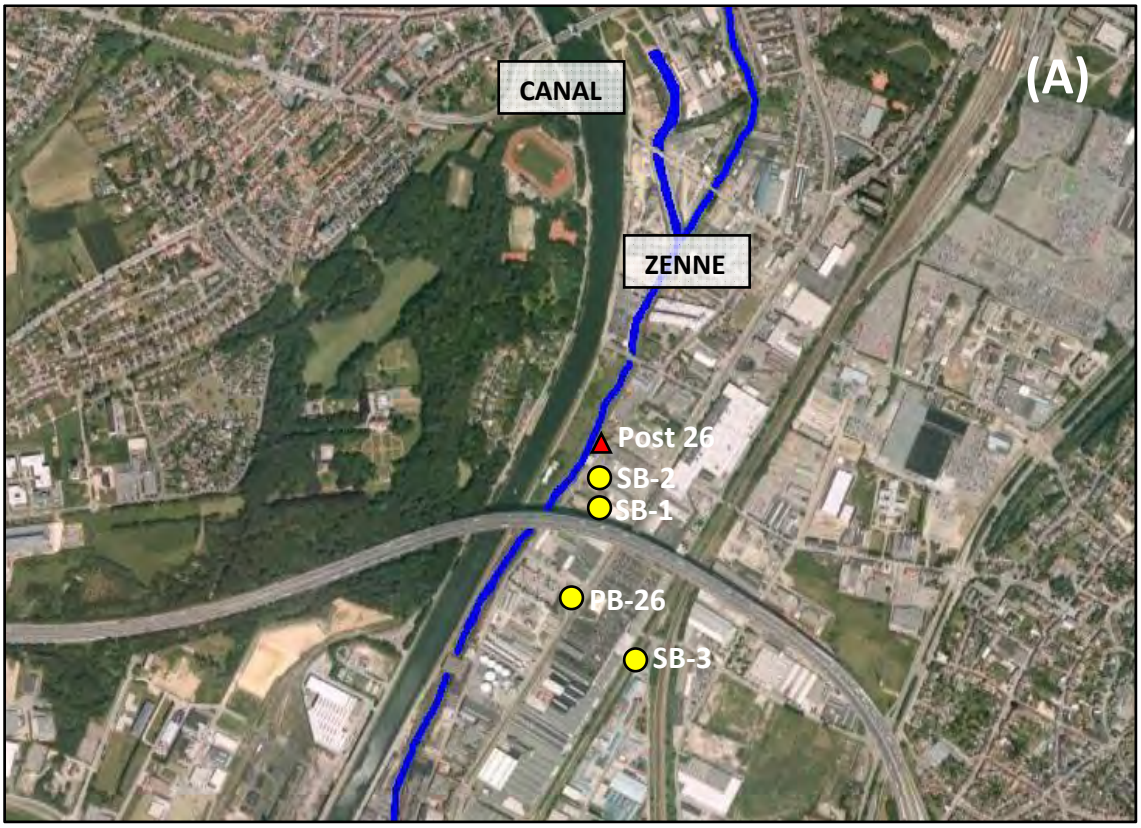

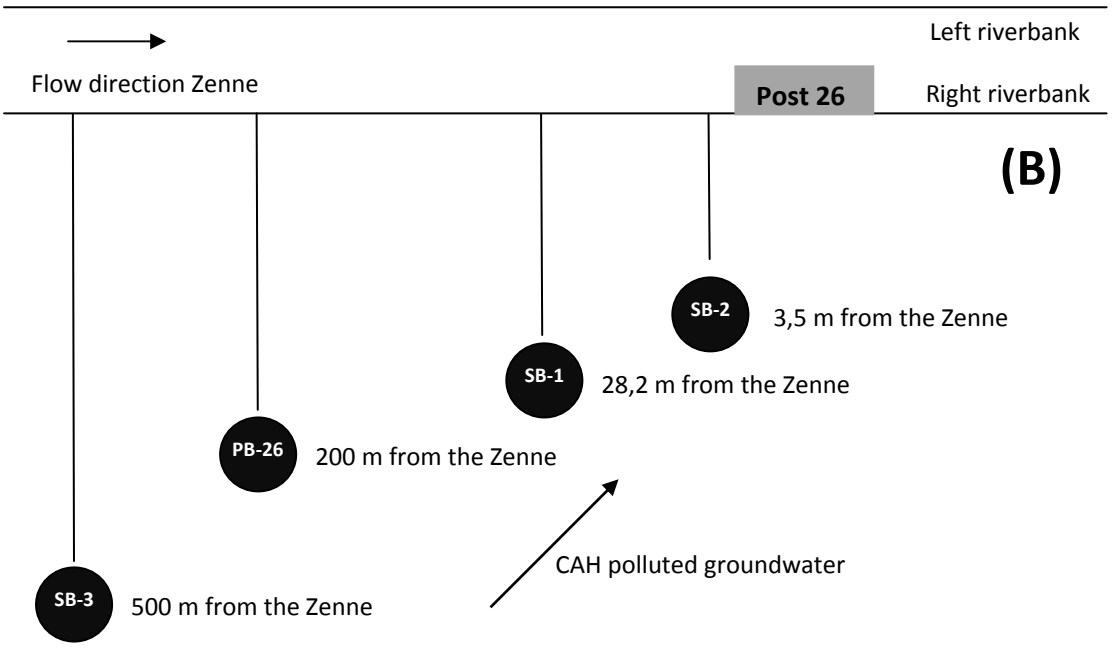

Figure 7.1. (A) Site map of Vilvoorde (Belgium) showing the River Zenne, the nearby canal, the location of the sampled monitoring wells (○) and the location of surface water and sediment collection (▲) (Google Maps, 2009). (B) Schematic overview of the sampled locations. Flow directions of the CAH plume and River Zenne are indicated by arrows.

From the collected groundwater and surface water, aliquots for chemical analyses were taken as follows: samples for analyses of CAHs and the dissolved hydrocarbons methane, ethene and ethane were both collected in duplicate into 10 mL headspace vials containing 0.1 mL concentrated H_3PO_4. Five millilitres samples were transferred into the vials and immediately closed using Teflon-lined caps. Samples for the inorganic parameters sulphate, nitrate and nitrite were collected in 30 mL plastic bottles. Moreover, 10 mL of water for cation analyses was filtered through a 0.45 µm sterile filter and brought to plastic vials containing 0.2 mL concentrated HNO_3. Finally, 10 mL samples were also filtered through a 0.45 µm sterile filter and transferred to a 50 mL plastic vial for dissolved organic carbon (DOC) analysis.

Once in the laboratory all the collected samples were stored at 4°C until its use in experiments. Samples for analyses of CAHs, methane, ethene and ethane were stored at 4°C and measured within two days after collection. All the other aliquots were also stored at 4°C, except samples for DOC analysis, which were stored at -20°C.

3.3. BATCH BIODEGRADATION TESTS

Batch microcosms were performed to investigate the *cis*-DCE biodegradation capacity in aquifer material collected from three different locations in the test area (SB-2, PB-26 and SB-3) (Figure 7.1). Biotic and abiotic control microcosms were prepared without addition of an external electron donor. Moreover, in the abiotic controls, microbial population was inhibited by adding formaldehyde (37%, Merck). Stimulation of *cis*-DCE degradation in the aquifer by addition of either lactate or molasses as electron source was studied, as well as the effect of adding sediments from River Zenne or an aqueous extract of these river sediments. All the experimental conditions were assayed *in duplo* and details are provided in Table 7.1.

Microcosm tests containing groundwater and aquifer material from each specified location were set-up to test three different experimental conditions: natural attenuation, abiotic control and lactate amendment (Table 7.1). Under an anaerobic atmosphere, aquifer material was collected from previous VC degradation tests performed under the same conditions that were studied in this new set of tests. The recovery of aquifer material from VC tests was performed by means of centrifugation and, when needed, new aquifer material was added. An amount of 37 g of well mixed recovered aquifer was suspended in 90 mL of fresh groundwater (from the same location of the aquifer material) in sterilized 160 mL serum bottles under anaerobic conditions.

Table 7.1. Details of batch microcosm test performed for the SB-2, PB-26 and SB-3 location samples.

Microcosm condition	Aquifer (g)[a]	Ground-water (mL)	Lactate ($mg \cdot L^{-1}$ C)[c]	Molasses ($mg \cdot L^{-1}$ C)[c]	Formal-dehyde (mL)	Sediment (g)	Sediment extract (mL)	Sediment extract centrifuged (mL)	Aquifer extract (mL)
Natural attenuation	37	90	-	-	-	-	-	-	-
Abiotic control	37	90	-	-	1	-	-	-	-
Groundwater control [b]	-	120	-	-	-	-	-	-	-
Lactate	37	90	380	-	-	-	-	-	-
Molasses [b]	37	90	-	380	-	-	-	-	-
Sediment	-	-	-	-	-	37	-	-	90
Sediment extract [b]	37	-	-	-	-	-	90	-	-
Centrifuged sediment extract [b]	37	-	-	-	-	-	-	90	-

[a] Weight in wet basis.

[b] Conditions tested only for the location PB-26.

[c] Units in $mg \cdot L^{-1}$ of carbon.

In addition, microcosm tests with homogenized river sediments instead of aquifer material and aquifer extract as the liquid phase were also prepared for each selected location (Table 7.1). The aquifer extract was prepared by suspending 125 g of aquifer material in 300 mL groundwater from the same location under an anaerobic atmosphere. The suspension was rotated during a week and afterwards it was sedimented overnight. The supernatant was used in the sediment conditions instead of groundwater.

Other additional four conditions were also tested for the PB-26 location: groundwater control and stimulation with molasses, sediment extract and centrifuged sediment extract (Table 7.1). Groundwater control was prepared without aquifer addition by filling with groundwater until the same level of others microcosms (i.e. maintaining the same headspace). The sediment extracts were prepared similarly to the aquifer extracts. In this case, an amount of 125 g of homogenized wet sediment was suspended in 300 mL of PB-26 groundwater. Sediment extract refers to the supernatant without sediment and the centrifuged sediment extract refers to the centrifugation of the supernatants without sediment pellet. By using sediment extract, DOC and CAH-degrading-bacteria are added to the microcosms, while by using centrifuged sediment extract, only DOC is added to the flasks.

Once all the microcosm tests were set-up, bottles were sealed with aluminium crimp caps containing Teflon-lined butyl-rubber septa (Alltech Associates Inc.). At this point, the appropriate amounts of lactate, molasses and formaldehyde were added to the tests. One millilitre of previous prepared anaerobic and sterile stock solutions of sodium lactate and molasses in mineral water was added to microcosms. It should be emphasized that these stock solutions were prepared in order to achieve a final total organic carbon (TOC) concentration in microcosms of 380 $mg \cdot L^{-1}$, which corresponded to the same amount of TOC available in tests amended with sediment extract.

All the microcosms were spiked with 6.5 $mg \cdot L^{-1}$ *cis*-DCE (67.1 $\mu mol \cdot L^{-1}$) (97%, Acros organics) and 3 $mg \cdot L^{-1}$ VC (48 $\mu mol \cdot L^{-1}$) (100%, Praxair NV). Afterwards, all the tests were vigorously shaken and set at 12°C overnight. At this point, nitrogen gas was added in the headspace of the bottles using a sterile syringe and samples for DOC measurement were withdrawn. In addition, CAHs and methane, ethene and ethane were analysed.

Microcosm tests were incubated in the dark at 12°C for 92 days and headspace samples were analysed at regular intervals to measure the concentration of CAHs and methane, ethene and

ethane. Each time the analysis was done, the flasks were previously spiked with 1 mL of nitrogen gas to prevent the entrance of oxygen into the bottles during analysis.

3.4. COLUMN OPERATION

Dynamic experiments were conducted in previously constructed 100 or 150 cm length, 4.2 cm inner diameter Plexiglass columns fitted with Teflon sampling ports at the inlet, outlet and along the height of the columns at 1, 2, 5 or 10 cm intervals (Hamonts, 2009). Sampling ports along the side of the columns were sealed by insertion of short pieces of stainless steel tubes closed at the end by welding.

Four 150 cm sediment columns (S1, S2, S3 and S4) had been assembled on site with black sand at the top and gray sand underneath. The top section of the columns (approximately 50 cm) was filled with Zenne surface water. Moreover, four 100 cm aquifer columns (A5, A6, A7 and A8) had been packed in the laboratory with homogenized aquifer fraction smaller than 1 cm (Hamonts, 2009). The columns were maintained at room temperature. A schematic overview of the columns is shown in Figure 7.2.

From October-November 2005 onwards, sediment and aquifer columns were continuously fed with groundwater that was monthly collected from the monitoring well SB-1 (Figure 7.1). Groundwater was pumped into the columns from collapsible TEDLAR bags (3.8 L, dual valve system, Cole-Parmer) that were wrapped with aluminium foil and stored in 100% nitrogen atmosphere nalophene bag. TEDLAR bags were filled without leaving headspace, by transferring about 1600 mL of groundwater into the bags in a nitrogen-purged glovebox (Don Whitley Scientific Ltd). Five millilitres samples for analyses of CAHs and methane, ethene and ethane were collected in duplicate into 10 mL headspace vials containing 0.1 ml concentrated H_3PO_4 immediately after filling the bags. Moreover, the dissolved oxygen (DO) concentration of groundwater was checked to assure that anaerobic conditions were maintained. Groundwater was pumped into the columns in an upward flow via a peristaltic multi-channel pump (Watson Marlow 205S, VWR).

As stated above, the top part of the river sediment columns was filled with surface water from River Zenne, which was continuously refreshed. Surface water was pumped into the columns at a flow rate of 45 $mL \cdot day^{-1}$ from 2 L glass bottle using a peristaltic pump (Watson Marlow 205S, VWR). The bottle was covered with aluminium foil and connected to a collapsible nalophane headspace bag filled with nitrogen gas. Moreover, the section of the columns containing Zenne water was also wrapped with aluminium foil to avoid algae growth.

Surface water infiltration into the riverbed was simulated in the column. The procedure was as follows: the sampling ports at 53.5 and 63.5 cm height were opened allowing surface water infiltration in the top 20 cm of the sediment layer while groundwater was removed at 53.5 cm. After several hours of surface water infiltration, the upward groundwater flow conditions were re-established.

Characteristics of the river sediment and aquifer columns are reported in Table 7.2. The porosity of the columns was determined from mass and volume measurements. Flow rates were measured by weighing the water volume of the waste reservoirs corresponding to a known time period and taking into account the density of water. Pore water velocity (v_{H2O}) was calculated using the following expression (Appelo and Postma, 2005):

$$v_{H2O} = \frac{J_w}{A \cdot \varepsilon} \tag{7.1}$$

in which J_w is the flow rate, A is the cross section area of the column and ε is the porosity.

Table 7.2. Properties of the river sediment and aquifer columns.

Column	Length (cm)[a]	Mass (g)[d]	d.m. (%)[b, d]	OM (% d.m.)[c, d]	Porosity (%)	Flow rate (mL·d^{-1})	Pore water velocity (cm·d^{-1})
Sediment columns							
S1	96.5	2899	80.0	0.14 (1.34)[e]	43	126.5	21.1
S2	86.5	2669	80.0	0.14 (1.34)[e]	45	48.4	7.8
S3	80.5	2461	80.0	0.14 (1.34)[e]	44	50.7	8.3
S4	77.0	2296	80.0	0.14 (1.34)[e]	43	52.7	8.8
Aquifer columns							
A5	93.5	2796	86.6	0.17	29	50.4	12.6
A6	93.5	2843	86.6	0.17	29	52.5	12.9
A7	93.5	2804	86.6	0.17	29	51.7	12.9
A8	87.5	2804	86.6	0.17	32	50.5	11.4

[a] Length of the river sediment and aquifer layer in columns.
[b] Dry matter content.
[c] Organic matter content (in % dry matter).
[d] Measurements performed during the set-up of the columns (Hamonts, 2009).
[e] The organic matter content differs between the gray and black sand in the sediment columns. The organic matter content of the black sand is reported in brackets.

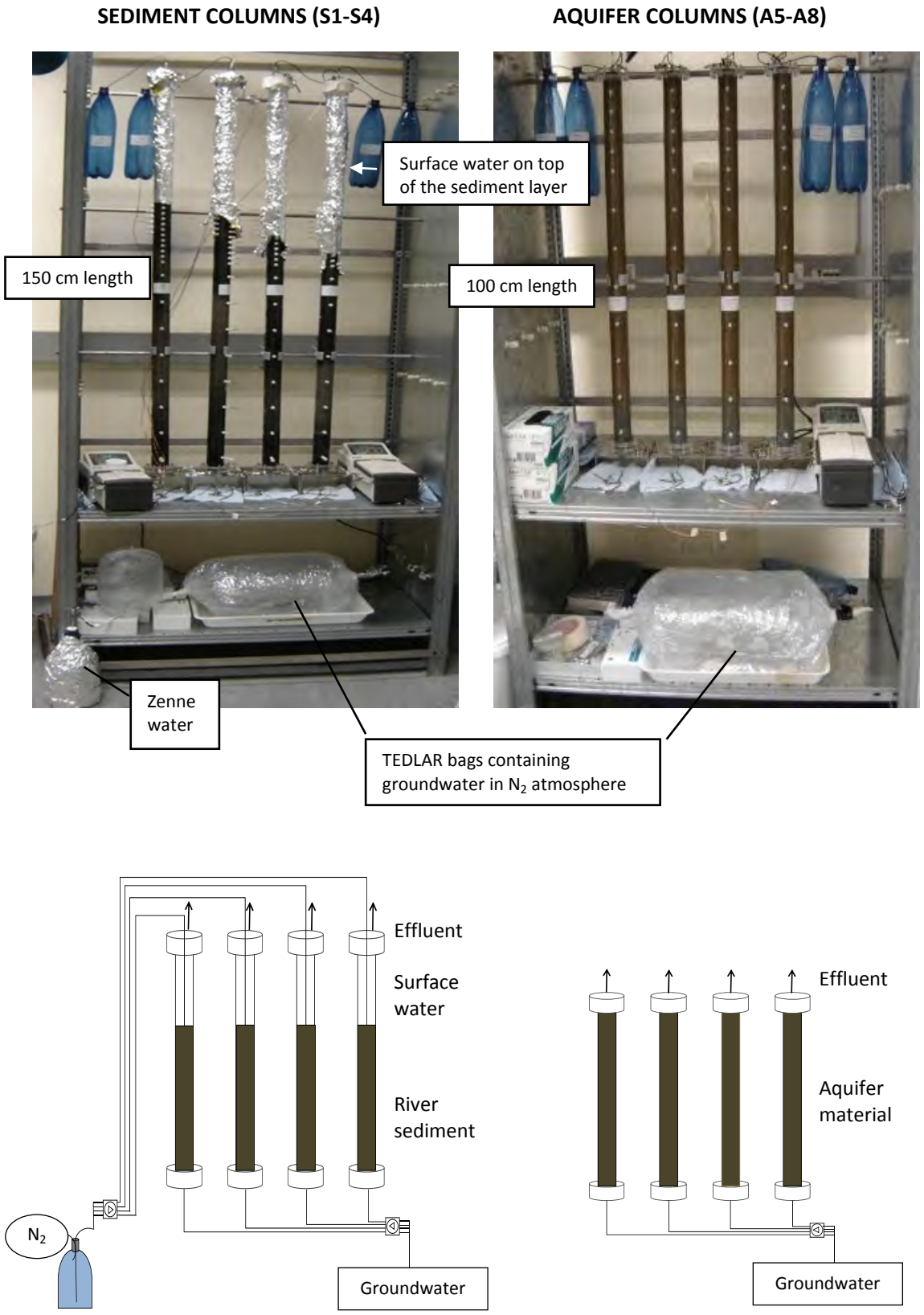

Figure 7.2. Pictures (top) and schematic diagram (bottom) of the Zenne sediment columns (left) and aquifer columns (right).

3.5. COLUMN STIMULATION PROCEDURE

In order to study the capacity to promote reductive dechlorination in sediment and aquifer columns, amendments with either sediment extract or lactate were carried out. A summary of the operation conditions tested in each column is provided in Table 7.3.

Table 7.3. Operation conditions of the river sediment and aquifer columns.

Column	Condition
S1	Natural attenuation
S2	Natural attenuation
S3	Stimulated with lactate[a]
S4	Natural attenuation
A5	Stimulated with sediment extract[a]
A6	Stimulated with lactate[a]
A7	Natural attenuation
A8	Natural attenuation

[a] Correspond to 3000 $mg \cdot L^{-1}$ TOC.

Sediment extract was prepared by suspending 300 g of homogenized Zenne River sediments in 300 mL SB-1 groundwater under anaerobic conditions. The suspension was maintained in rotation during a week. At this point, it was sedimented overnight. The supernatant was used to stimulate the A5 aquifer column. Lactate was added to A6 and S3 columns from an anaerobic solution of sodium lactate in SB-1 groundwater containing the same TOC concentration as the prepared sediment extract (i.e. 3000 $mg \cdot L^{-1}$ TOC).

The stimulation procedure was as follows: the inlet of the columns was closed and 100 mL of sediment extract, lactate solution or SB-1 groundwater was pumped into the proper columns using a syringe pump at a flow rate of 1 $mL \cdot min^{-1}$. It should be mentioned that columns not being stimulated with lactate or sediment extract (i.e. S1, S2, S4, A7 and A8) were amended with SB-1 groundwater in order to reproduce the same conditions that were taking place in the stimulated columns. Once the stimulation was performed, groundwater upflow conditions were re-established for one week before starting the sampling campaign. This period corresponded to the time needed for the added stimulating solutions to reach the top of the columns.

3.6. COLUMN SAMPLING

Columns were sampled at different heights from top to bottom to minimize disturbance of the upward flow. During the sampling, the outlet of the column was closed and pore water samples were collected by removing the welded stainless steel tube from the selected sampling ports and inserting autoclaved sampling devices. These devices consisted of large needles of 1.6x40 mm, filled with glass wool to prevent sand blocking of the device, connected to fine needles of 0.6x25 mm with flexible Viton tube. The plastic ends of the needles were removed in order to assemble the sampling devices. The large needle was inserted into the selected sampling port of the column, whereas the fine needle was inserted into pre-weighted 10 mL headspace vial containing 0.1 mL concentrated H_3PO_4 and closed with Teflon-lined caps. These sampling vials had previously been flushed with nitrogen gas to prevent oxygen infiltration into the columns during sampling. Moreover, air from the vials was removed before sampling to allow pore water to enter.

The vials were attached to the columns for a total period of about 2.5 h to collect samples for CAHs or methane, ethene and ethane. This period corresponded to the time interval at which 5 mL groundwater was pumped into the columns. The vials were disconnected from the columns by extracting the needle from the liquid phase to avoid escape of volatile gases. The sampling volume was adjusted to 5 mL by extracting pore water from the vials or by adding mineral water to the liquid phase.

The influent of the columns was sampled by connecting vials to sterilized sampling devices. In this case, sampling devices consisted in a Viton tube attached to the stainless steel tube that enter the column at one end, and to a fine needle of 0.6x25 mm at the other end. The column inlet and outlet were closed during the influent sampling.

Moreover, at the beginning and the end of the column sampling campaign, groundwater samples for analyses of CAHs and methane, ethene and ethane were collected from the TEDLAR bags. The sampling was performed by extracting groundwater with gastight syringes (10 mL, Hamilton #1010) equipped with a 1-way Luer lock adaptor (Alltech) at a sampling port situated before the peristaltic pump.

3.7. ANALYTICAL METHODS

In groundwater, surface water and column pore water samples, CAHs concentrations were analysed using a Thermo Finnigan Trace GC-MS equipped with a DB5-MS column (60 m length, 0.25 mm id and 0.25 µm film thickness, J&W Scientific). Detection limits of the method were between 3 and 4 $\mu g \cdot L^{-1}$. Methane, ethene and ethane concentrations were measured using a Varian GC-FID (CP-3800) equipped with a Rt-U plot column (30 m length, 0.32 mm id and 3 µm film thickness, J&W Scientific). The detection limits were 0.5 $\mu g \cdot L^{-1}$.

Headspace analyses of the microcosm tests were performed using a Varian GC-FID (CP-3800) equipped with a Rt-U plot column (as described above) for the detection of methane, ethene and ethane or with a split-splitless injector followed by a Rt-X column (30 m length, 0.53 mm id and 3 µm film thickness, Restek) and a DB-1 column (30 m length, 0.53 mm id and 5 µm film thickness, J&W Scientific) for analyses of CAHs. Detection limits were 5 $\mu g \cdot L^{-1}$. At regular intervals, headspace samples of 400 or 250 µL were taken from the microcosms by a headspace autosampler (CombiPal CTC Analytics) for analyzing respectively CAHs and methane, ethene and ethane.

DOC was determined as the difference in total dissolved carbon and dissolved inorganic carbon using a C-mat 5500 (Ströhlein Instruments), according to the method NBN EN 1484.

DO was determined using a micro-cathode oxygen electrode connected to a model 781b oxygen meter (Strathkelvin Instruments). The standard error for oxygen measurement in a reference aerobic medium was ± 0.07 $mg \cdot L^{-1}$.

For sediment and aquifer samples, the dry matter content was determined after drying the material overnight at 105°C. The organic carbon content of homogenized sediments was calculated as the loss of ignition at 550°C during 4 h.

Concentrations of sulphate, nitrate and nitrite were analysed by ion chromatography using a Dionex DX-120 ion chromatograph equipped with a Dionex AS14A column, conform to method NBN EN ISO 10304. Detection limits of all the anions measured were between 0.02 $mg \cdot L^{-1}$ for nitrite and 0.25 $mg \cdot L^{-1}$ for nitrate. Concentrations of cations were analysed by inductively coupled argon plasma spectroscopy using Thermo Elemental Iris Intrepid ICP-AES-XUV (Thermo Fischer Scientific). The detection limits of all the cations analysed were between 0.014 and 0.03 $mg \cdot L^{-1}$.

4. RESULTS AND DISCUSSION

4.1. PHYSICOCHEMICAL CHARACTERIZATION OF GROUNDWATER AND ZENNE WATER

Field parameters and chemical characterization of sampled groundwater and surface water are indicated in Table 7.4. It should be mentioned that these results are from a point sampling campaign performed in October 2008. However, when comparing the obtained results with previous monitoring information (October 2005-June 2007), reported by Hamonts (2009), no significant differences were observed, indicating that the measured parameters are rather stable over time in the selected area.

Table 7.4. Physicochemical characteristics of groundwater and surface water at the Zenne site recorded in the sampling campaign from October 2008.

Monitoring location →	**Groundwater**				**Zenne water (post 26)**
Parameter ↓	**SB-2**	**SB-1**	**PB-26**	**SB-3**	
Field parameters					
Groundwater depth (m)	3.2	2.8	2.4	1.4	-
Temperature (°C)	14.3	12.9	15.6	15.9	15.7
Conductivity (µS·cm^{-1})	1356	1011	1548	1502	952
pH	7.4	7.2	7.4	7.1	8.5
DO (mg·L^{-1})	0.28	0.20	0.40	0.60	5.90
ORP (mV)	-17	-17	-16	-27	- 6
Chemical analyses					
cis-DCE (µg·L^{-1})	<D.L. [a]	33.5	<D.L.	6446.8	<D.L.
VC (µg·L^{-1})	412.4	872.3	71.6	3419.9	<D.L.
1,1-DCA (µg·L^{-1})	9.7	20.1	<D.L.	92.7	<D.L.
CA (µg·L^{-1})	39.1	<D.L.	<D.L.	<D.L.	<D.L.
Methane (µg·L^{-1})	703.3	376.4	290.0	495.6	19.7
Ethene (µg·L^{-1})	71.4	4.5	73.8	56.1	<D.L.
Ethane (µg·L^{-1})	47.4	5.7	4.5	13.9	<D.L.
Chloride (mg·L^{-1})	115	57	113	80	61
Sulphate (mg·L^{-1})	183	122	294	469	73
Nitrate (mg·L^{-1})	<D.L.	<D.L.	<D.L.	<D.L.	16
Nitrite (mg·L^{-1})	<D.L.	<D.L.	<D.L.	<D.L.	<D.L.
Fe (mg·L^{-1})	6.9	3.3	11	23	0.1
Mn (mg·L^{-1})	0.4	0.2	1.0	1.4	0.1
DOC (mg·L^{-1})	1.0	2.5	0.5	0.9	7.1

[a] <D.L: below detection limit.

Physicochemical parameters measured *in situ* demonstrated reductive conditions in the groundwater (DO concentrations ranged 0.2-0.6 $mg \cdot L^{-1}$ and ORP values were between -27 and -16 mV). In contrast, reducing conditions did not prevail in the Zenne surface water, where a DO concentration up to 5.90 $mg \cdot L^{-1}$ was measured. Nevertheless, before the sanitation of the surface water upstream of the test area (March 2007), strong reducing conditions were measured in the Zenne (DO concentration below 3 $mg \cdot L^{-1}$) (Hamonts, 2009).

CAHs were detected in all the collected groundwater samples, whereas concentrations in Zenne surface water were below the detection limits (Table 7.4). *cis*-DCE was present in SB-1 and SB-3 monitoring wells, with a concentration up to 6446.8 $\mu g \cdot L^{-1}$ (66.5 $\mu mol \cdot L^{-1}$) in the latter. The degradation product VC was observed in all the monitoring wells; however, it was again higher in the SB-3 well, with a concentration up to 3419.9 $\mu g \cdot L^{-1}$ (54.7 $\mu mol \cdot L^{-1}$). With regard to chlorinated ethanes, 1,1-DCA was observed in SB-2, SB-1 and SB-3 wells, whereas CA was only detected in SB-2. Moreover, the non-toxic end products ethene and ethane were observed in all the groundwater samples. The presence of VC, ethene and ethane indicate the biodegradation of the CAHs in the groundwater.

The presence of methane in groundwater samples demonstrated highly reducing methanogenic conditions, which are favourable for reductive dechlorination (Table 7.4). Furthermore, methane was also detected in surface water (19.7 $\mu g \cdot L^{-1}$), but before the sanitation of the water, concentrations up to 192 $\mu g \cdot L^{-1}$ were measured in the test area by Hamonts (2009).

In groundwater and surface water samples, low DOC concentrations were measured (Table 7.4). However, again, the low DOC content in surface water is due to the sanitation of water, before March 2007 concentrations up to 70 $mg \cdot L^{-1}$ DOC were observed (Hamonts, 2009).

4.2. EVALUATION OF *cis*-DCE BIODEGRADATION POTENTIAL OF THE ZENNE RIVER SEDIMENT AND AQUIFER IN BATCH TESTS

The intrinsic *cis*-DCE biodegradation capacity of aquifer material from three different sampled locations (SB-2, PB-26 and SB-3) was tested in microcosm experiments containing *cis*-DCE and VC contaminated groundwater from the same locations. In addition, the stimulation of the biodegradation potential by adding external carbon sources (i.e. lactate or molasses), river sediments or an extract of these sediments was also investigated.

Reductive dechlorination of *cis*-DCE and VC was only observed in the microcosm tests amended with Zenne sediments, an extract of the river sediments, lactate or molasses (Figure 7.3). Addition of river sediment resulted in a complete reductive dechlorination of initial *cis*-DCE and VC to non-toxic ethene within 47 d in the three studied locations. The same time was required to reductive dechlorinate *cis*-DCE and VC to ethene in tests from PB-26 amended with sediment extract, whereas in tests fed with centrifuged sediment extract, the complete *cis*-DCE and VC degradation took place after 56 d. In the lactate- and molasses- amended conditions from PB-26 tests, a complete *cis*-DCE and VC removal was also attained within 47 and 56 days, respectively. Nevertheless, these results do not agree with the profiles obtained in the lactate-amended conditions from SB-2 and SB-3 microcosms, where complete dechlorination of *cis*-DCE and VC could not be achieved within the 92 days of the experiment. Differences in lactate-amended conditions from the three different studied locations could be due to a different abundance of halorespiring bacteria in the tests. No evidence was obtained for this speculation since the microbial community composition was not monitored in the beginning and during the microcosm tests.

In all the stimulated microcosm tests, biodegradation of *cis*-DCE caused a temporarily increase of the VC concentration, followed by its reductively dechlorination to non-toxic ethene (Figure 7.3). However, the mass balance (sum of all chlorinated ethenes and degradation products ethene and ethane) was not constant throughout the experiments, and most of the times suddenly decreased due to the disappearance of ethene. Mass losses have also been described in previous laboratory and *in situ* tests (Hamonts, 2009). Microbial transformation of ethene or abiotic processes probably caused these mass losses.

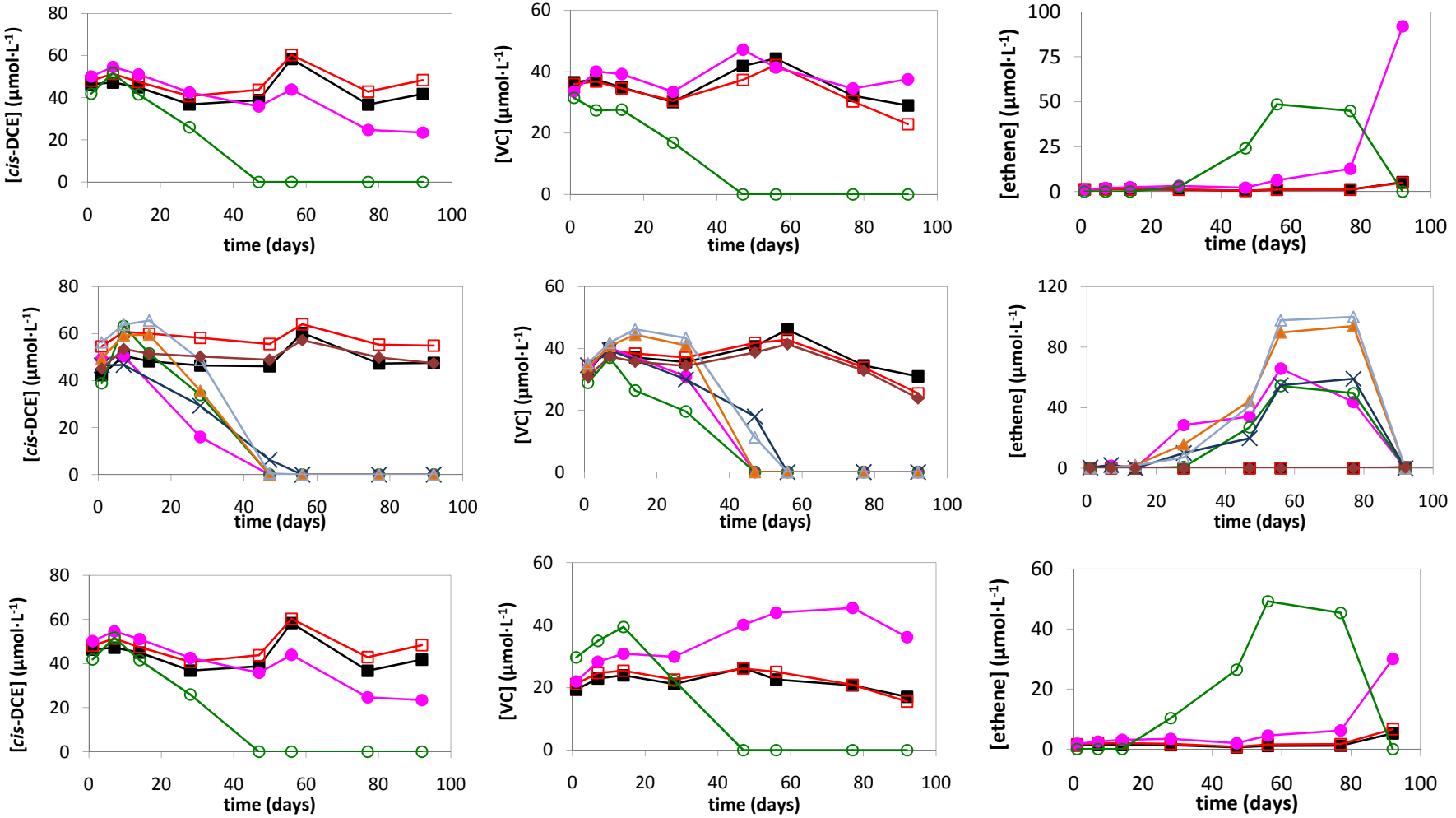

Figure 7.3. Profiles of *cis*-DCE, VC and ethene concentrations for SB-2 (top), PB-26 (middle) and SB-3 (bottom) microcosm tests under natural conditions (□), in the abiotic control (■), in groundwater control (◆) and under the effect of stimulating factors: lactacte (●), river sediment (○), molasses (×), sediment extract (▲) and centrifuged sediment extract (△). Data points are the average of duplicates.

Since no sorption of chlorinated ethenes was demonstrated in the performed control tests, the removal of these contaminants can be attributed to biodegradation. It is well known that the degradation kinetics of microbial mediated reactions is complex and might depend on several biochemical and environmental factors (Clement *et al.*, 2000). Nevertheless, in many cases biodegradation rates of CAHs are approximated using first-order kinetics (Wiedemeier *et al.*, 1998). First-order CAHs degradation can be described by the following equation:

$$\frac{d[CAH]}{dt} = -K_{CAH} \cdot [CAH] \tag{7.2}$$

where $[CAH]$ is the concentration of CAHs at time *t* and K_{CAH} is the first-order rate constant, which represents the overall CAH attenuation rate. Solving this differential equation yields:

$$[CAH] = [CAH]_0 \cdot e^{-t \cdot K_{CAH}} \tag{7.3}$$

where $[CAH]_0$ is the initial concentration of CAHs (*t* = 0).

It should be emphasized that the use of the first-order kinetics is appropriate when the biodegradation rate is solely controlled by the CAH concentration. When more than one substrate is limiting the microbial degradation rate or when the microbial population is increasing or decreasing over time, the first-order approximation is not appropriate (Wiedemeier *et al.*, 1998).

According to equation 7.3, first-order biodegradation rate constants for *cis*-DCE were calculated from the slope of the regression line in a ln-linear plot of the measured *cis*-DCE concentration versus time in microcosm tests. Note that the lag phase before the onset of *cis*-DCE was ignored for the calculation. Results are detailed in Table 7.5. It can be observed that similar biodegradation rate constants were obtained in microcosms amended either with river sediment, sediment extracts or molasses, whereas main differences were seen in the lactate-amended SB-2 and SB-3 microcosm tests. As stated above, biodegradation in lactate conditions of SB-2 and SB-3 tests was slow and not complete within the 92 days experiment. VC biodegradation rate constants were not calculated due to the low number of samples measured during its attenuation.

Table 7.5. First-order *cis*-DCE biodegradation rate constants estimated from microcosms tests.

Microcosm	First order *cis*-DCE biodegradation rate (d^{-1})		
	SB-2	**PB-26**	**SB-3**
Lactate	0.010	NA[a]	0.0014
Molasses	-	0.270	-
Sediment	0.272	0.280	0.274
Sediment extract	-	0.280	-
Centrifuged sediment extract	-	0.295	-

[a] NA: not available, calculation was not performed due to the limited measurements within the period of *cis*-DCE attenuation.

Methane production was only observed in the stimulated tests (data not shown). Specially, the sediment-amended microcosms presented the most pronounced production of methane, reaching concentrations up to 324.3, 313.3 and 313.9 $mg \cdot L^{-1}$ after 77 days in SB-2, PB-26 and SB-3 tests, respectively.

Concerning chlorinated ethanes, it is important to note that 1,1-DCA was only significantly present in groundwater from the monitoring well SB-3 (Table 7.4). Hence, microcosm tests containing aquifer material from this location presented 1,1-DCA (about 90 $\mu g \cdot L^{-1}$), except the sediment-amended test, where the preparation of the aquifer extract probably caused the loss of this compound by volatilization. Nevertheless, biodegradation of 1,1-DCA was not observed in any of the microcosm tests. Concentrations remained constant not only in the abiotic and biotic control, but also in the lactate-amended test. Moreover, no presence of degradation products (CA and ethane) was observed (data not shown).

Overall, microcosm tests clearly showed that aquifer material did not drive the *cis*-DCE and VC reductive dechlorination process without the addition of an external source of electron donors. In contrast, the capacity of Zenne sediments to stimulate CAHs dechlorination was demonstrated. The difference in CAHs biodegradation potential of aquifer and river sediments can be attributed to differences in the abundance of CAH-degrading bacteria. Previous studies demonstrated that *Dehalococcoides* were present in aquifer samples at lower densities than in sediment samples (Hamonts, 2009). This reason could explain not only the no biodegradation in aquifer microcosms under natural conditions, but also the lag phase detected when adding an external carbon source. This lag phase would reflect the time needed to increase the halorespiring population to attain perceptible degradation.

Furthermore, differences in the organic matter content between both aquifer and sediments could also be related to the variable biodegradation capacity. DOC results of aquifer extracts from the three sampled locations revealed concentrations lower than 12 $mg \cdot L^{-1}$ DOC, whereas in sediment extracts TOC and DOC concentrations were up to 381 and 103 $mg \cdot L^{-1}$, respectively. Other authors have suggested that hydrogen produced from the fermentation of natural organic substrates in the river sediment could serve as electron donor for the dechlorination of CAHs (Himmelheber *et al.*, 2007; McCarty, 1997).

4.3. EVALUATION OF CAHs BIODEGRADATION POTENTIAL OF THE ZENNE RIVER SEDIMENT AND AQUIFER IN COLUMN TESTS

The intrinsic CAHs reductive dechlorination potential of eutrophic Zenne sediments and the aquifer adjacent to the river was also studied by means of column experiments. In addition, the capacity to stimulate CAH degrading microorganisms by lactate or sediment extract addition, as well as by surface water infiltration into the sediments, was investigated. Throughout this work, three different sampling campaigns were performed in the columns after their proper stimulation. Main results obtained in sediment and aquifer columns are detailed in this section. Furthermore, abiotic processes occurring in columns are investigated.

4.3.1. Sediment columns

During the first two years of columns operation, reductive dechlorination of *cis*-DCE and VC to non-toxic ethene was observed in the sediment columns (Hamonts, 2009). However, this biodegradation pattern was not observed in the sampling campaigns of the sediment columns performed throughout this work, where the decrease in *cis*-DCE and VC concentrations were not accompanied by a proportional increase in the concentration of the microbial degradation product ethene. Thus, it is suggested in this work that abiotic processes were likely taking place. Results of chlorinated ethenes and the degradation products ethene and ethane obtained in the lactate-amended column (S3) are shown in Figure 7.4A. It can be observed that the mass balance (sum of all chlorinated ethenes and degradation products) was not constant along the height of the column; this mass loss corroborates the presence of abiotic processes mainly effecting the VC concentration. Similar profiles of chlorinated ethenes and degradation products were obtained in the sediment columns under natural conditions (S1, S2 and S4) where, again, VC was not further reduced to ethene and mass losses were observed along the columns (data not shown). These results seem to indicate that the addition of lactate in the

sediment columns did not improve the dechlorination potential of *cis*-DCE and VC. Although these results showed apparent VC attenuation along the columns, they may be misinterpreted due to the effect of abiotic processes.

In contrast, reductive dechlorination of 1,1-DCA to CA was observed in all the sediment columns. Results from sediment column S3 are shown in Figure 7.4B. Again, no significant differences were observed in the biodegradation of 1,1-DCA in the lactate-amended column (S3) compared to the columns running at the same flow rate under natural conditions (S2 and S4) (data not shown). From these results it can be suggested that the hydrogen produced from the fermentation of natural organic substrates present in the river sediments (Himmelheber *et al.*, 2007; McCarty, 1997) was sufficient to drive reductive dechlorination of CAHs in sediment columns, and that the addition of lactate did not improve the intrinsic biodegradation potential.

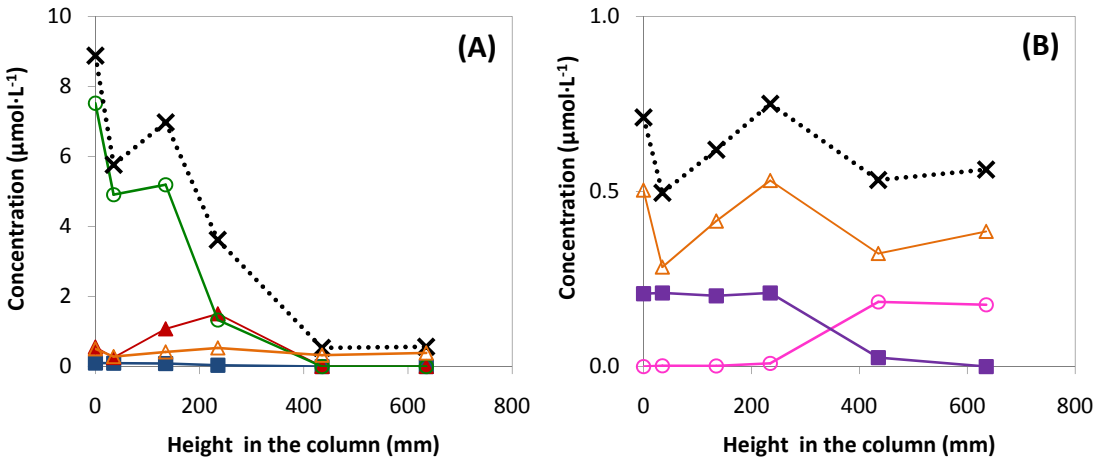

Figure 7.4. (A) Profiles of *cis*-DCE (■), VC (○), ethene (▲) and ethane (△) and (B) reductive dechlorination of 1,1-DCA (■) to CA (○) but not ethane (△) along the height of the sediment column S3 (stimulated with lactate). The total mass balance of the presented compounds is depicted in each graph (×).

The reductive dechlorination pattern of 1,1-DCA to CA has been reported for halorespiring *Dehalobacter* species (Grostern and Edwards, 2006). It is noteworthy that the biodegradation of 1,1-DCA started between 23.5 and 43.5 cm height in all the sediment columns and that similar results were obtained in previous work (Hamonts, 2009). This behaviour could reflect the inhibition of the 1,1-DCA degrading microorganisms by the presence of the co-contaminants VC and *cis*-DCE. Grostern and Edwards (2006) investigated the biodegradation of 1,1,1-TCA and TCE in batch tests inoculated with halorespiring *Dehalococcoides* and *Dehalobacter* species, and they reported that 1,1-DCA was only dechlorinated to CA by *Dehalobacter* species after the chlorinated ethenes were fully converted into ethene by

Dehalococcoides species. However, in contrast to the study of Grostern and Edwards (2006), biodegradation of 1,1-DCA in this project occurred in the presence of up to 1.2 µmol·L^{-1} *cis*-DCE and 14.8 µmol·L^{-1} VC. The presence of lower concentrations of chlorinated ethenes in the influent groundwater (14.3 µmol·L^{-1} versus 30 to 300 µmol·L^{-1} in the study of Grostern and Edwards) or acquired resistance of the 1,1-DCA degrading microorganisms to elevated concentrations of VC and *cis*-DCE over time in the columns, could be reasons for the mentioned discrepancy. Kaseros *et al.* (2000) observed in column tests a similar acclimation over time of PCE-degrading microorganisms to elevated concentrations of carbon tetrachloride, of which the biodegradation product chloroform is a known inhibitor of PCE biodegradation.

Differences in the production of methane were observed in the columns. In the three sampling campaigns, methane concentration in the lactate-amended column (S3) increased along the column reaching higher concentrations than in the columns under natural conditions (S1, S2 and S4). On average, the methane concentration in S3 reached a maximum concentration of about 2200 µg·L^{-1}, whereas in S1, S2 and S4 methane concentration was only up to 43 µg·L^{-1}.

The low groundwater residence time applied in the column S1 by increasing the flow rate resulted in a larger column length needed to complete removal of CAHs. On average, S1 could only remove 47% *cis*-DCE and 35% 1,1-DCA within 73.5 cm, whereas in the columns with a lower flow rate (S2, S3 and S4) the complete removal of *cis*-DCE and 1,1-DCA was observed within the same height (data not shown).

As previously described, the influence of surface water infiltration was tested in the sediment columns, simulating the Zenne water infiltration into the riverbed. It is known that the infiltration of surface water dilutes the upwelling CAHs concentrations, but also it could provide organic material to fermenting microbial populations in the sediments, resulting in an increased production of hydrogen for reductive dechlorination reactions. Results from the sampling campaign performed after the surface water infiltration showed no differences on the CAH degradation potential in S2, S3 and S4. In contrast, in S1 a higher reductive dechlorination was achieved, with 75% *cis*-DCE and 54% 1,1-DCA versus 47% *cis*-DCE and 35% 1,1-DCA removal within 73.5 cm (data not shown).

The observed loss in biodegradation potential of chlorinated ethenes in sediment columns and the increasing attenuation by abiotic processes with time might be explained by the formation of preferential flow paths. The long period of columns operation (three years) could have

contributed to the formation of these preferential flow paths, decreasing the availability of electron donors for dechlorinating microorganisms in the vicinity of contaminants and reducing the overall biodegradation capacity of the system. Himmelheber *et al.* (2007) observed a loss of dechlorination and methanogenic activity in sediment columns over time and the need to provide new electron donors to achieve complete biodegradation. In contrast to the results of Himmelheber *et al.* (2007), in this work, the addition of lactate did not improve the biodegradation potential and abiotic processes were seen to play the main role in the removal of VC.

4.3.2. Aquifer columns

Results from aquifer columns demonstrated that under natural conditions no reductive dechlorination of *cis*-DCE and VC to non toxic ethene was taking place. These results are in accordance with the previous work performed in the columns (Hamonts, 2009). Moreover, results clearly reflected that abiotic processes were taking place. In columns under natural conditions (A7 and A8) and in the lactate-amended column (A6), a decrease in VC concentrations not accompanied by ethene production was observed in the first layers of the columns. In addition, an increase in VC concentrations in pore liquid samples of the top layers of the columns was also observed. Therefore, not only mass losses, but also increases, were detected inside the columns (Figure 7.5). It should be stressed that during the first three years of columns operation, it had already been demonstrated that a removal of 34% VC over 1 m aquifer columns was attributed to abiotic processes, since no increase in the biodegradation products ethene or ethane was detected (Hamonts, 2009). Nevertheless, no accumulation of VC in the top layers of aquifer columns had ever been detected before. It is suggested in this work that volatilization in the first layers and accumulation at the top layers of the aquifer columns or sorption/desorption of VC might be taking place inside the columns. In contrast, in column A5, fed with sediment extract, a decrease in VC concentration together with an increase of ethene was observed. Moreover, no increase of VC was observed along the column, indicating that biodegradation was the main process taking place (Figure 7.6A).

Regarding chlorinated ethanes, results demonstrated that reductive dechlorination of 1,1-DCA to CA was also only taking place in the sediment extract-amended column (A5) (Figure 7.6B). Nevertheless, as it can be observed in Figure 7.6, mass losses in both cases (i.e. chlorinated ethenes and ethanes) were observed along the height of the column A5

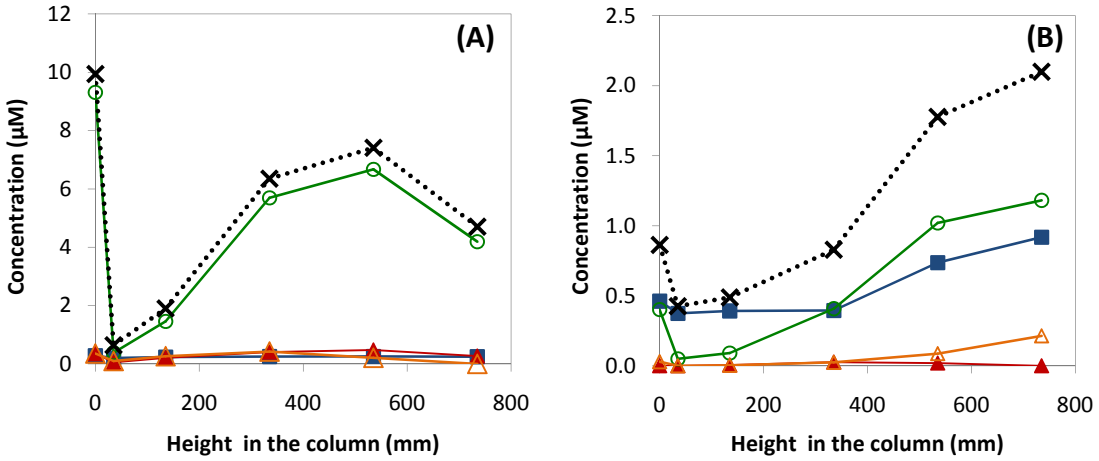

Figure 7.5. Profiles of *cis*-DCE (■), VC (○), ethene (▲) and ethane (△) obtained along the height of the aquifers column (A) A8 (natural attenuation) and (B) A6 (stimulated with lactate). The total mass balance of the presented compounds is depicted in the graph (×).

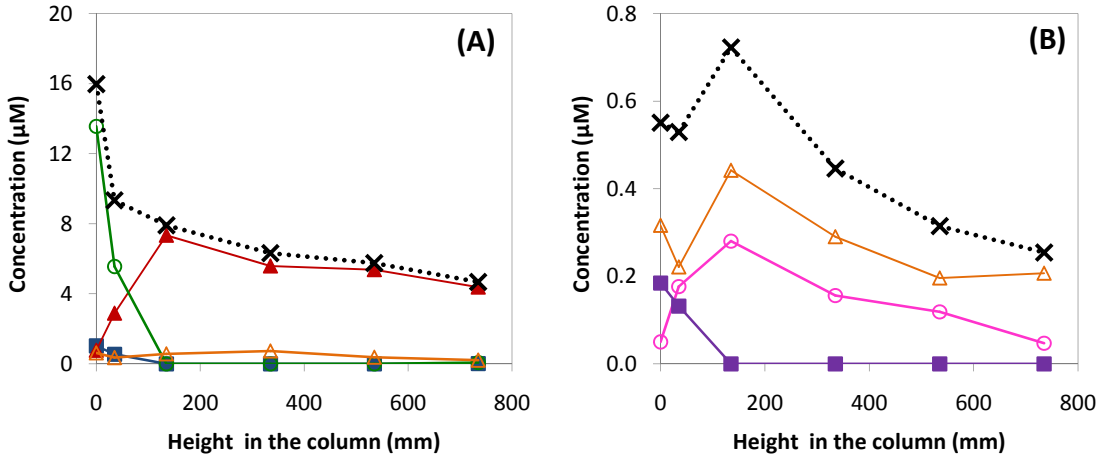

Figure 7.6. (A) Reductive dechlorination of *cis*-DCE (■) and VC (○) to ethene (▲) but not ethane (△) and (B) reductive dechlorination of 1,1-DCA (■) to CA (○), but not ethane (△) along the height of the aquifer column A5 (stimulated with sediment extract). The total mass balance of the presented compounds is depicted in the graph (×).

Methanogenesis was highly more pronounced in the column amended with sediment extract (methane concentration up to 925.7 µg·L^{-1}) compared to the lactate-amended column (methane concentration up to 29.7 µg·L^{-1}) and the columns under natural conditions (methane concentration up to 22.6 µmol·L^{-1}).

The amendment with lactate could not drive the reductive dechlorination of CAHs in the aquifer column A6. These results together with the low production of methane seem to indicate a lack of microbial activity in the column. The absence of biodegradation of *cis*-DCE and VC is in agreement with qPCR analyses previously performed by Hamonts (2009), in which *Dehalococcoides* was not detected in aquifer columns. Nevertheless, the amendment with

sediment extract could promote CAHs biodegradation since the sediment extract fed the aquifer material not only with organic matter, but also with indigenous CAH-degrading bacteria from the Zenne sediments. Previous qPCR analyses revealed the presence of *Dehalobacter* in the aquifer columns, although biodegradation of 1,1-DCA was never observed. This can be explained because *cis*-DCE and VC were not reduced in the aquifer columns due to the lack of *Dehalococcoides* and their presence may inhibit biodegradation of 1,1-DCA by the detected *Dehalobacter* populations (Grostern and Edwards, 2006).

4.3.3. Study of abiotic processes in sediment and aquifer columns

As stated above, abiotic processes played an important role in chlorinated ethenes and ethanes attenuation in sediment and aquifer columns. Sorption of contaminants in sediment and aquifer material is a function of the interstitial water concentration in which they are exposed to and sorption factors that affect the distribution coefficient (Kd) of the material. The Kd of an organic compound is defined as the ratio of the sorbed contaminant concentration (C_s) to the dissolved contaminant concentration (C_l). In materials containing an organic carbon content higher than 0.1%, Kd can be approximated by the product of the organic carbon content (foc) of the material and the organic-carbon/water partitioning coefficient (KOC) of the contaminant (Schwarzenbach and Westall, 1981):

$$Kd = \frac{C_s}{C_l} = KOC \cdot foc \tag{7.4}$$

Considering that the fraction of total organic carbon in the gray sand at the bottom of sediment columns was calculated to be 0.0014 (in the set-up of the columns, Table 7.2) and that reported Koc values for VC range from 0.4 to 56 L·kg^{-1} (U.S. Environmental Protection Agency, 1995; Wiedemeier *et al.*, 1998), 0.1 to 7.8% of the VC concentration of influent groundwater would be expected to be sorbed to the gray material. Sorption of *cis*-DCE and 1,1-DCA to the gray sand, taking into account Koc values of 49 and 33 L·kg^{-1}, respectively (Wiedemeier *et al.*, 1998), would result in a sorbed concentration of 6.9% and 4.6% of the *cis*-DCE and 1,1-DCA inlet groundwater concentrations, respectively. Furthermore, in the black sand on the top of sediment columns, the calculated sorbed concentrations were between 0.5 and 75% VC, 65.7% *cis*-DCE and 44.2% 1,1-DCA. Concerning the aquifer columns, sorbed concentrations were calculated to be between 0.1-9.5% VC, 8.3% *cis*-DCE and 5.6% 1,1-DCA.

From these results it can be concluded that, except for the black sand in sediment columns, sorption of *cis*-DCE, VC and 1,1-DCA would not play a main role in the attenuation of these contaminants. Nevertheless, the increase in VC concentration observed in the top layers of aquifer columns could be due to its desorption. The VC drop in the first layers of sediment (Figure 7.5A) could have induced the VC desorption to maintain equilibrium conditions, allowing greater aqueous phase concentrations. Volatilization of CAHs, specially VC for its higher vapour pressure, could have also contributed to the decrease in the contaminants concentration with height in the columns. Although this process is unlikely in saturated systems, it should be mentioned that several samplings of packed material were performed for molecular analyses. These samplings could have caused the formation of holes inside the packed columns allowing VC volatilization. It is hypothesized that the combination of these processes may have contributed to the high observed VC attenuation in the columns.

Overall, column tests corroborated the higher CAH biodegradation potential of the eutrophic Zenne sediments compared to the aquifer material adjacent to the river. Nevertheless, the abiotic processes inside the columns were seen to become more important with time in the removal of CAHs, specially of chlorinated ethenes, both in the sediment and aquifer columns.

5. CONCLUSIONS

Microcosm tests performed with aquifer soil and groundwater from three different locations (SB-2, PB-26 and SB-3) in the test area demonstrated that aquifer could not trigger *cis*-DCE and VC dechlorination without the addition of an electron source.

High potential to promote dechlorination of CAHs was demonstrated in microcosm tests amended with Zenne sediments regardless of the *in situ* groundwater used. Moreover, the use of sediment extracts could also drive complete dechlorination of *cis*-DCE and VC to non-toxic ethene. Lactate and molasses were also demonstrated to be suitable electron donors to achieve dechlorination of *cis*-DCE and VC in the aquifer microcosms.

In sediment columns, reductive dechlorination of 1,1-DCA to CA was observed. However, attenuation of the chlorinated ethenes *cis*-DCE and VC could not be linked to halorespiration, since no production of the end product ethene was detected. Moreover, the addition of lactate in a sediment column did not improve reductive dechlorination of CAHs. It is suggested in this work that the long time period of columns operation contributed to the formation of

preferential flow paths that reduce the biodegradation capacity and caused that abiotic processes played the main role in VC attenuation.

The effect of infiltrating surface water into the top sediment layers could not be evaluated in sediment columns, except in column S1 with a higher flow rate, where it resulted in a higher biodegradation potential. In addition, residence time in sediment columns could be related to the length needed to remove CAHs.

In aquifer columns under natural conditions, no biodegradation of VC, *cis*-DCE or 1,1-DCA was observed. Moreover, the amendment with lactate did not drive reductive dechlorination of CAHs in aquifer columns. This result could be related to the non-detectable levels of *cis*-DCE- and VC-reducing *Dehalococcoides* spp. and the inhibition of detected *Dehalobacter* spp. by the chlorinated ethenes (Hamonts, 2009). In contrast, the amendment with sediment extract could promote reductive dechlorination of these CAHs.

Abiotic processes played an important role in the attenuation of CAHs inside the columns, specially in the attenuation of chlorinated ethenes. Theoretical sorption was calculated to be negligible in aquifer columns and in the section filled with gray sand of the sediment columns. However, it was seen to be important in the black sand section of sediment columns. Although it could not be experimentally evaluated, a combination of volatilization and sorption are hypothesized to play important roles in the attenuation of chlorinated ethenes inside the columns.

6. REFERENCES

Appelo, C.A.J. and Postma, D. 2005. Geochemistry, groundwater and pollution. A.A. Balkema Publishers. Amsterdam, The Netherlands.

Bradley, P.M. and Chapelle, F.H. 1998. Microbial mineralization of VC and DCE under different terminal electron accepting conditions. *Anaerobe*, 4, 81-87.

Bronders, J., Touchant, K., Van Keer, I., Patyn, J. and Provoost, J. 2007. The characterization of contamination and the role of hydrogeology in the risk management of a mega brownfield site *In:* Fifth Congress of the International Association of Hydrologists, Groundwater and Ecosystems, eds. Ribeiro, L., Chambel, A. and Condesso de Melo, M.T., Lisbon, Portugal.

Brunke, M. and Gonser, T. 1997. The ecological significance of exchange processes between rivers and groundwater. *Freshwater Biology*, 37, 1-33.

Clement, T.P., Johnson, C.D., Sun, Y.W., Klecka, G.M. and Bartlett, C. 2000. Natural attenuation of chlorinated ethene compounds: model development and field-scale application at the Dover site. *Journal of Contaminant Hydrology*, 42, 113-140.

Conant, B., Cherry, J.A. and Gillham, R.W. 2004. A PCE groundwater plume discharging to a river: influence of the streambed and near-river zone on contaminant distributions. *Journal of Contaminant Hydrology*, 73, 249-279.

Chapman, S.W., Parker, B.L., Cherry, J.A., Aravena, R. and Hunkeler, D. 2007. Groundwater-surface water interaction and its role on TCE groundwater plume attenuation. *Journal of Contaminant Hydrology*, 91, 203-232.

Ellis, P.A. and Rivett, M.O. 2007. Assessing the impact of VOC-contaminated groundwater on surface water at the city scale. *Journal of Contaminant Hydrology*, 91, 107-127.

Feris, K.P., Ramsey, P.W., Frazar, C., Rillig, M.C., Gannon, J.E. and Holben, W.E. 2003. Structure and seasonal dynamics of hyporheic zone microbial communities in free-stone rivers of the western United States. *Microbial Ecology*, 46, 200-215.

Fischer, A.J., Rowan, E.A. and Spalding, R.F. 1987. VOCs in groundwater influenced by large scale withdrawals. *Ground Water*, 25, 407-414.

Grostern, A. and Edwards, E.A. 2006. A 1,1,1-trichloroethane-degrading anaerobic mixed microbial culture enhances biotransformation of mixtures of chlorinated ethenes and ethanes. *Applied and Environmental Microbiology*, 72, 7849-7856.

Hamonts, K. 2009. Structure and pollutant-degrading activity of the microbial community in eutrophic river sediments impacted by discharging chlorinated aliphatic hydrocarbon-polluted groundwater. Ph.D. thesis. Faculteit Bio-ingenieurswetenschappen. Katholieke Universiteit Leuven, Leuven (Belgium).

Hamonts, K., Kuhn, T., Maesen, M., Bronders, J., Lookman, R., Kalka, H., Diels, L., Meckenstock, R.U., Springael, D. and Dejonghe, W. 2009. Factors Determining the Attenuation of Chlorinated Aliphatic Hydrocarbons in Eutrophic River Sediment Impacted by Discharging Polluted Groundwater. *Environmental Science & Technology*, 43, 5270-5275.

Himmelheber, D.W., Pennell, K.D. and Hughes, J.B. 2007. Natural attenuation processes during in situ capping. *Environmental Science & Technology*, 41, 5306-5313.

Kuhn, T.K., Hamonts, K., Dijk, J.A., Kalka, H., Stichler, W., Springael, D., Dejonghe, W. and Meckenstock, R.U. 2009. Assessment of the Intrinsic Bioremediation Capacity of an Eutrophic River Sediment Polluted by Discharging Chlorinated Aliphatic Hydrocarbons: A Compound-Specific Isotope Approach. *Environmental Science & Technology*, 43, 5263-5269.

LaSage, D.M., Sexton, J.L., Mukherjee, A., Fryar, A.E. and Greb, S.F. 2008. Groundwater discharge along a channelized Coastal Plain stream. *Journal of Hydrology*, 360, 252-264.

Lendvay, J.M., Dean, S.M. and Adriaens, P. 1998. Temporal and spatial trends in biogeochemical conditions at a groundwater-surface water interface: Implications for natural bioattenuation. *Environmental Science & Technology*, 32, 3472-3478.

McCarty, P.L. 1997. Microbiology - Breathing with chlorinated solvents. *Science*, 276, 1521-1522.

Pusch, M., Fiebig, D., Brettar, I., Eisenmann, H., Ellis, B.K., Kaplan, L.A., Lock, M.A., Naegeli, M.W. and Traunspurger, W. 1998. The role of micro-organisms in the ecological connectivity of running waters. *Freshwater Biology*, 40, 453-495.

Schwarzenbach, R.P. and Westall, J. 1981. Transport of non-polar organic-compounds from surface-water to groundwater. Laboratory sorption studies. *Environmental Science & Technology*, 15, 1360-1367.

Smatlak, C.R., Gossett, J.M. and Zinder, S.H. 1996. Comparative kinetics of hydrogen utilization for reductive dechlorination of tetrachloroethene and methanogenesis in an anaerobic enrichment culture. *Environmental Science & Technology*, 30, 2850-2858.

Smith, J.W.N. 2005. Groundwater-Surface water interactions in the hyporheic zone. Environment Agency Science Report SC030155/SR1, Environment Agency. Bristol, UK.

Squillace, P.J., Moran, M.J., Lapham, W.W., Price, C.V., Clawges, R.M. and Zogorski, J.S. 1999. Volatile organic compounds in untreated ambient groundwater of the United States, 1985-1995. *Environmental Science & Technology*, 33, 4176-4187.

U.S. Environmental Protection Agency. 1995. Contaminant specific fact sheets, Volatile organic chemicals. Technical version: EPA 811-F-95-004-T, EPA. Washington, DC.

Wiedemeier, T.H., Swanson, M.A., Moutoux, D.E., Kinzie Gordon, E., Wilson, J.T., Wilson, B.H., Kampbell, D.H., Haas, P.E., Miller, R.N., Hansen, J.E. and Chapelle, F. 1998. Technical protocol for evaluating natural attenuation of chlorinated solvents in ground water. U.S. Environmental Protection Agency, Report EPA/600/R-98/128, EPA, Washington, DC.

Yang, Y.R. and McCarty, P.L. 1998. Competition for hydrogen within a chlorinated solvent dehalogenating anaerobic mixed culture. *Environmental Science & Technology*, 32, 3591-3597.

Chapter 8

GENERAL CONCLUSIONS AND PERSPECTIVES

1. GENERAL CONCLUSIONS

ENHANCED DENITRIFICATION

1. Microcosm and dynamic experiments with soil and groundwater from a nitrate-contaminated aquifer in Argentona, Catalunya (Spain) demonstrated that an amendment with an electron donor was required to promote denitrification in the aquifer material.

2. Enhanced heterotrophic and autotrophic denitrification resulted in a high nitrate removal in microcosm experiments. The main difference between both processes was the denitrification rate; the heterotrophic denitrification was faster than the autotrophic process.

3. Organic carbon limitation was consistently associated with partial denitrification and significant nitrite accumulation in laboratory-scale experiments.

4. In a continuous-flow soil column amended with glucose, a nitrate load up to 18 $mg \cdot L^{-1} \cdot h^{-1}$ could be successfully denitrified from groundwater. However, the bioremediation process resulted in hydrodynamic changes, mainly reduction of porosity and increase of dispersivity.

MODELLING

5. A multiple-Monod model describing the organic carbon consumption by oxygen- and nitrate-based respiration together with the growth and decay of an heterotrophic facultative microbial population could successfully explain experimental data obtained in microcosm batch tests with aquifer material at 17°C.

6. The model was properly calibrated with a microcosm test consisting of four consecutive denitrification tests. The optimal estimated parameters were consistent with published values.

7. The model was extended to explain enhanced denitrification in the dynamic experiment by adding transport processes and nitrite kinetics. Simulation results could predict the growth of heterotrophic bacteria in the first layers of the soil column and the transient accumulation of nitrite inside the column. However, the model could not be calibrated with the performed experiment.

MOLECULAR TECHNIQUES

8. Real-time PCR assays targeting 16S rRNA and *nosZ* genes were conducted in soil and groundwater samples from the denitrification column experiment. Results revealed that the amendment with glucose to promote denitrification resulted in a rapid increase of the total eubacterial population and, specially, of denitrifiers.

9. DGGE analysis of 16S rRNA in soil and groundwater samples from the denitrification column demonstrated changes on the diversity of the indigenous eubacterial population from aquifer due to the glucose addition. The band pattern in soil samples from the bottom of the column (close to the water inlet) was significantly different from initial soil samples, corroborating that main microbial activity was in the first layers of the soil column.

10. The sequencing of prominent 16S rRNA DGGE bands corroborated the increase of denitrifiers among the eubacterial population present in the soil column amended with glucose.

CAHs BIOREMEDIATION

11. Bioremediation of *cis*-DCE and VC was investigated by means of microcosm and column tests containing River Zenne sediments or aquifer material collected within the CAH plume adjacent to the river (Vilvoorde, Belgium). Results indicated a higher intrinsic microbial CAH-degradation potential in the Zenne sediments compared to the aquifer adjacent to the river.

12. Amendments with different electron donors, such as lactate and molasses, promoted the reductive dechlorination of CAHs in aquifer microcosm tests.

13. Abiotic processes, such as sorption/desorption and volatilization, played an important role in the attenuation of CAHs inside sediment and aquifer columns. The long-term performance of the columns was linked to the increase of the importance of such abiotic processes.

2. PERSPECTIVES

1. Future work should be addressed on the execution of larger scale denitrification tests, such as pilot-scale tests and eventually field demonstration, to better study the factors influencing on the denitrification process as well as the negative effects which could be derived from an *in situ* implementation, such as hydrodynamic changes or spatial nitrite accumulation.

2. A next step in modelling should be the proper calibration of the kinetic and stoichiometric parameters involved in the two step denitrification model. This would allow to understand and predict the effects of the transient accumulation of nitrite in enhanced denitrification processes. Furthermore, the dynamic model should be tested with specially-designed dynamic experiments.

3. Messenger ribonucleic acid (mRNA) analysis would be the next step towards understanding the different factors influencing not only on the microbial population density but also on the denitrifying genes expression in response to different conditions.

4. Concerning CAHs bioremediation in the studied site, future research should focus on studying different strategies to increase the efficiency of the Zenne sediments to act as effective biobarriers for the CAH-polluted groundwater. For example, a possible strategy would be the *in situ* capping of the sediment to prolong the groundwater residence time in the riverbed, which could be tested in column experiments like the ones applied in this work.